Adaptive Hybrid Control for Robust Global Phase Synchronization of Kuramoto Oscillators

Alessandro Bosso, Ilario Azzollini, Simone Baldi, Luca Zaccarian

Adaptive Hybrid Control for Robust Global Phase Synchronization of Kuramoto Oscillators

Alessandro Bosso[1], *Member, IEEE*, Ilario A. Azzollini[2], Simone Baldi[3], *Senior Member, IEEE*, and Luca Zaccarian[4], *Fellow, IEEE*

***Abstract*— A distributed controller is designed for the robust adaptive global phase synchronization of a network of uncertain second-order Kuramoto oscillators with a leader system, modeled as an autonomous nonlinear exosystem that communicates the reference signals only to a subset of the oscillators. We propose an adaptive strategy, only assuming knowledge of upper bounds on the unknown oscillators parameters, that exploits a hybrid hysteresis mechanism to obtain global synchronization despite the well-known topological obstructions with the phases (which evolve on the unit circle). A distributed observer of the leader exosystem is key to overcoming these topological obstructions combined with the generic graph topology we consider. Leveraging the results of hybrid systems theory, including reduction theorems, Lyapunov techniques, and properties of ω-limit sets, we prove global convergence of the phases to the leader reference and robust global asymptotic stability of the closed-loop dynamics, despite the presence of an adaptive control law.**

***Index Terms*— Kuramoto oscillators, distributed control, hybrid control, adaptive control, robustness.**

I. Introduction

A. Networks of Kuramoto oscillators

SYNCHRONIZATION and coordination phenomena are ubiquitous in several application domains, including physics, engineering, biology, and social sciences. In this context, special attention is given to the collective behavior of networks of interacting oscillators such as those described by the Kuramoto model [1]. This model is capable of capturing with appealing mathematical simplicity complex nonlinear phenomena such as those emerging in power networks [2], [3] or connectivity patterns in the human brain [4], [5]. The original Kuramoto model was characterized by first-order phase dynamics. Second-order models involve an additional angular frequency state, where each oscillator has its own inertia [3], [6]. Recent extensions include the third-order Kuramoto model [7], inspired by the transient behavior of power networks, or the generalization of the phase state space given by the Kuramoto model on Stiefel manifolds [8], capable of including in a unified framework both the classical model and more complex structures such as the Lohe model [9].

In general, synchronization of Kuramoto oscillators may occur with or without a control input affecting the network. Concerning the *uncontrolled scenario*, significant efforts have been dedicated to studying the impact of couplings (either the network topology or the intensity of connections) on the synchronization properties of the trajectories [10]–[15]. In the *controlled scenario*, the emphasis is on finding an appropriate input to achieve synchronization in an artificially engineered network, typically assuming that a controller is located at each node [16], [17]. Representative engineering applications with this structure include microgrids [18] or planar circular formations [19], [20]. When rotations are involved, as in attitude control of rigid bodies, Kuramoto-like higher-dimensional dynamics arise [21], [22].

This work focuses on leader-follower synchronization, also known as pacemaker-based synchronization [23]. This control scenario involves a leader system dictating the desired behavior of the network. However, the leader's reference signals are not directly available to all nodes in the graph.

A challenge in achieving leader-follower synchronization is that the controller of each node should employ only locally available quantities received from its neighbors, according to a communication graph topology. Then, significant challenges emerge from the goal of obtaining synchronization despite disturbances, measurement noise or model uncertainties (requiring robustness), and unknown parameters (requiring adaptation). Moreover, when aiming at global properties, challenging fundamental obstructions exist, as discussed next.

This work was supported in part by the European Union's Horizon Europe research and innovation programme via the Marie Skłodowska-Curie Grant Agreement No 101104404 - IMPACT4Mech, by the Natural Science Foundation of China via grant 62073074, by the MUR via grant DOCEAT, CUP E63C22000410001, No 2020RTWES4, and by the ANR via grant OLYMPIA, No ANR-23-CE48-0006.

[1]A. Bosso (corresponding author) is with the Department of Electrical, Electronic, and Information Engineering (DEI), University of Bologna, Italy. Email: alessandro.bosso@unibo.it

[2]I. A. Azzollini is with the R&D Launch Team, E80 Group, Italy. Email: ilario.azzollini92@gmail.com

[2]S. Baldi (corresponding author) is with School of Mathematics, Southeast University, Nanjing, China. Email: simonebaldi@seu.edu.cn

[3]L. Zaccarian is with LAAS-CNRS, Université de Toulouse, and the Department of Industrial Engineering, University of Trento, Italy. Email: zaccarian@laas.fr

B. Obstructions to global synchronization

It has been well recognized in the literature that the non-Euclidean nature of the state space of a Kuramoto model is the main obstruction to achieving global asymptotic convergence to the leader's reference phase. When representing the phase of each oscillator as an element of the unit circle $\mathbb{S}^1$, the ensemble of N phase angles is an element of the N-torus $\mathbb{T}^N$ [24], which is a bounded set. This leads to the advantage that phase synchronization can be reformulated as the attractivity of a compact set. Although this formulation is beneficial for control design, the N-torus is a non-Euclidean set, meaning that synchronization cannot be handled with the tools used in linear synchronization by consensus. Indeed, globally solving the consensus problem on $\mathbb{T}^N$ with generic undirected connected graphs, possibly including cycles, is significantly complicated by the possible generation of stable attractors not corresponding to synchronization [24]. Thus, the attention has been often restricted to the special case of acyclic graph topologies, as in [21].

In addition, the topological properties of a non-contractible space (i.e., not diffeomorphic to any Euclidean space) pose significant obstacles to *global stabilization through continuous feedback*. For instance, the continuous-time algorithms (and their corresponding discrete-time versions) in [24] lead to multiple equilibria in the state space, where only one of them corresponds to the desired configuration. The same issue is shared by several applications involving rotations: for example, in the above-mentioned context of attitude control, only *almost global* results can be achieved with continuous laws for control [25] and observation [26].

In recent years, it has been shown that robust global stabilization can be achieved on non-contractible spaces through dynamic *hybrid* (instead of continuous) feedback [27]. Meaningful results have been proposed, e.g., for unit quaternions [27] through hysteresis-based techniques and for the N-sphere [28] via synergistic potential functions. Some efforts have also been dedicated to the unit circle [29]. However, all of the above solutions have been developed in a single-agent scenario and in the absence of uncertain dynamics. One of the first attempts to present hybrid feedback in a multi-agent setting can be found in [21], for the special case of acyclic graph topology. An interesting distributed global quaternion synchronization solution for generic graphs, proposed in [22], combines a sliding-mode distributed observer and a hybrid stabilizer. Nonetheless, due to the presence of static discontinuities, the global synchronization properties are not robust to uncertainties and measurement noise.

Despite the progress in the field, to the best of the authors' knowledge, a control scheme is still missing to achieve robust adaptive global leader-follower synchronization of uncertain Kuramoto oscillators for generic undirected and connected graphs.

C. Main contributions of this work

The goal of this work is to achieve *robust adaptive global asymptotic leader-follower phase synchronization* in a generic connected network of second-order Kuramoto oscillators, i.e., to globally asymptotically track a phase reference trajectory produced by a leader without precise information of the parameters of the oscillators, except for known upper bounds.

To overcome the above-mentioned fundamental obstructions, we adopt a hybrid dynamical systems approach following the formalism in [30] with special care for the well-posedness of the closed-loop dynamics. Well-posedness allows us, among other things, to benefit from the use of powerful Lyapunov-based stability analysis tools, such as the hybrid invariance principle from [30, Ch. 8], and reduction theorems from [31]. Our distributed controller comprises the following components embedded in each node: (a) a distributed observer for obtaining a local estimate of the leader's reference; indeed, the reference may be not directly available to all the nodes in large engineered communication networks due to technological limitations [20] (which forbid the scenario where the leader can send the reference to all the nodes, solvable through local tracking controllers); (b) a hybrid synchronizer used to track the locally estimated reference and to enable phase synchronization in a global sense; (c) an adaptive mechanism that achieves asymptotic phase synchronization in the presence of the parametric uncertainties of the heterogeneous oscillators.

The original contributions of this work can be summarized as follows.

(i) By virtue of our distributed observer combined with invariance and reduction theorems, we succeed in *globally solving the consensus problem on $\mathbb{T}^N$ with generic undirected connected graphs also including cycles, with a leader that communicates only with a subset of the graph nodes*. Therefore, with our approach, we avoid the above-discussed issues associated with undesirable stable attractors [24] and overcome the acyclic graph assumption of existing works [21]. In our general setting, the observer-based architecture is essential to decouple the global synchronization problem on $\mathbb{T}^N$ into N global synchronization problems on $\mathbb{S}^1$.

(ii) The leader system, representing a generator of the reference signals available to part of the network, is taken as a novel nonlinear second-order system (*exosystem*) far more general than those employed in the literature [22], [32]. Indeed, we allow for a feedback interconnection between the phase and frequency subsystems under a mild Lipschitz bound on the nonlinearities at the right-hand side, whereas the existing literature only handles cascaded interconnections. The only fundamental connection of the exosystem with the physical oscillators is that the phase reference evolves on the unit circle $\mathbb{S}^1$, to be compatible with the phases of the Kuramoto oscillators. In the analysis of our distributed observer, we show that classical ISS-small-gain tools [33, Ch. 10], applied to this novel class of exosystems, ensure global asymptotic distributed estimation and, more

importantly, provide explicit tuning rules depending on the graph connectivity and the Lipschitz bounds of the novel leader dynamics.

(iii) To ensure compatibility with the parameter adaptation mechanism, for the synchronizer design we revisit and extend the hysteresis-based hybrid controllers originally proposed in [27] to deal with the topological obstructions associated with the unit circle. Indeed, we augment these controllers with a first-order filter so that the stabilizing input does not change across jumps, a key property for interlacing the hybrid synchronizer with the continuous-time adaptation commented below. This approach may reveal useful in independent works where discontinuous inputs might cause undesirable Lyapunov increase at jumps (see, e.g., the issues in [34, Fig. 2]).

(iv) With our adaptation mechanism, we prove two meaningful properties for the closed-loop system without requiring persistency of excitation: existence of a *robustly globally asymptotically stable compact attractor*; global asymptotic convergence of all phases to the reference exosystem. The first property, which may sound atypical as compared to standard results in the adaptive literature, is an original contribution of this work. This result is unlocked by embedding the overall dynamics in a hybrid inclusion [30]. Then, the powerful characterization of ω-limit sets of well-posed hybrid systems, together with a simple dead-zone-based projection mechanism for keeping the parameter estimates in a compact set, enables proving the existence of such a compact globally asymptotically stable attractor. To the best of the authors' knowledge, no similar result is found in the adaptive literature, where no analysis tools for hybrid inclusions are typically used.

(v) By globally asymptotically stabilizing a compact set for the well-posed closed-loop system, our formulation ensures from [30, Ch. 7] intrinsic *robustness properties* that imply graceful performance degradation in the presence of measurement noise and small persistent unmodeled disturbances (the so-called semiglobal practical property). Among other things, such robustness guarantees ensure that the closed-loop stability properties are also preserved (semiglobally and practically) under a sample-and-hold implementation of the hybrid feedback [35]. Such robustness features cannot be proven with discontinuous solutions such as those in [22].

A preliminary version of this study has been published in [36]. In this paper, we improve [36] in several directions. First, [36] considers the simplified case of known parameters of the Kuramoto oscillators. Moreover, [36] considers a simplified cascaded exosystem structure as in [22], [32], in place of the more general class of exosystems discussed above in item **(ii)**.

The paper is organized as follows. Sections II and III are dedicated, respectively, to formulating the model and presenting a formal statement of the control problem. Then, Section IV defines the distributed observer and provides a detailed stability analysis of the estimation error dynamics. Section V introduces the hybrid controller for reference tracking, along with a preliminary stability analysis in conditions of global knowledge of the reference signal. The results of the previous sections are collected and exploited in Section VI, which presents the overall stability analysis based on reduction theorems. In Section VII, we validate the theoretical results through numerical simulations that confirm the effectiveness of the proposed solution. Section VIII concludes the article.

Notation

$\mathbb{R}$ and $\mathbb{Z}$ denote the sets of real and integer numbers, while $\mathbb{R}_{\geq 0} \coloneqq [0, \infty)$. The transpose of real-valued vectors and matrices is denoted with $(\cdot)^\top$, while $\otimes$ indicates the Kronecker matrix product. For any integer $n \geq 1$, I_n is the identity matrix of dimension n and $\mathbf{1}_n \in \mathbb{R}^n$ is the vector of all ones. With column vectors v and w, the notation (v, w) indicates the concatenated vector $[v^\top \ w^\top]^\top$. $\mathrm{diag}(a_1, \ldots, a_n)$ denotes the block-diagonal matrix with diagonal elements a_i, $i \in \{1, \ldots, n\}$. Finally, $\underline{\sigma}(\cdot)$ denotes the smallest singular value of matrices.

1) Graph Theory: An undirected graph of order N is defined as $\mathcal{G} \coloneqq \{\mathcal{V}, \mathcal{E}\}$, where $\mathcal{V} \coloneqq \{1, \ldots, N\}$ is a finite non-empty set of nodes and $\mathcal{E} \subseteq \mathcal{V} \times \mathcal{V}$ is a set of non-ordered pairs of nodes, called edges. For each $i \in \mathcal{V}$, $\mathcal{N}_i \coloneqq \{j \in \mathcal{V} : (i, j) \in \mathcal{E}\}$ is the set of neighbors of i. An undirected graph $\mathcal{G}$ is connected if, taken any arbitrary pair of nodes (i, j), $i, j \in \mathcal{V}$, there is a path from i to j. Given a leader node not included in $\mathcal{V}$, we denote with $\mathcal{T} \subseteq \mathcal{V}$ the set of target nodes, i.e., the set of nodes that receive information from the leader.

For an undirected graph $\mathcal{G}$ with target nodes $\mathcal{T}$, the adjacency matrix $A = [a_{ij}] \in \mathbb{R}^{N \times N}$ is defined as $a_{ij} = a_{ji} = 1$ if $(i, j) \in \mathcal{E}$, $i \neq j$, and $a_{ij} = 0$ otherwise; the Laplacian matrix $L = [l_{ij}] \in \mathbb{R}^{N \times N}$ is defined as $l_{ii} = \sum_j a_{ij}$ and $l_{ij} = -a_{ij}$ if $i \neq j$, while the target matrix $T = [\tau_{ij}] \in \mathbb{R}^{N \times N}$ is a diagonal matrix such that $\tau_{ii} = 1$ if $i \in \mathcal{T}$ and $\tau_{ii} = 0$ otherwise. Finally, the matrix $B \coloneqq L + T$ is denoted as leader-follower matrix. For an undirected and connected graph $\mathcal{G}$ with $\mathcal{T} \neq 0$ (equivalently, with $T \neq 0$), B is positive definite [37].

2) Hybrid Dynamical Systems: A hybrid dynamical system $\mathcal{H} \coloneqq (C, F, D, G)$ can be compactly described as [30]:

$$\mathcal{H} : \begin{cases} \dot{x} \in F(x), & x \in C \\ x^+ \in G(x), & x \in D \end{cases} \tag{1}$$

where $x \in \mathbb{R}^n$ is the state, $C \subset \mathbb{R}^n$ is the flow set, $F : \mathbb{R}^n \rightrightarrows \mathbb{R}^n$ is the flow map, $D \subset \mathbb{R}^n$ is the jump set, and $G : \mathbb{R}^n \rightrightarrows \mathbb{R}^n$ is the jump map. A solution of (1) can either flow according to the differential inclusion $\dot{x} \in F(x)$ when $x \in C$, or jump according to the difference inclusion $x^+ \in G(x)$ when $x \in D$. Below, we recall definitions and results from [30, Ch. 7] that will be used for robust adaptive synchronization.

First, we provide global versions of $\mathcal{KL}$ and robust $\mathcal{KL}$ asymptotic stability [30, Defs. 7.10 and 7.18]. A compact

set $\mathcal{A} \subset \mathbb{R}^n$ is said to be *globally $\mathcal{KL}$ asymptotically stable* for system (1) if there exists a function $\beta \in \mathcal{KL}$ such that

$$|x(t,j)|_{\mathcal{A}} \leq \beta(|x(0,0)|_{\mathcal{A}}, t+j), \quad \text{for all } (t,j) \in \operatorname{dom} x, \tag{2}$$

for every solution x of (1). Then, we say that a compact set $\mathcal{A} \subset \mathbb{R}^n$ is *globally robustly $\mathcal{KL}$ asymptotically stable* if there exists a continuous function $\rho : \mathbb{R}^n \to \mathbb{R}_{\geq 0}$, positive on $\mathbb{R}^n \backslash \mathcal{A}$, such that $\mathcal{A}$ is globally $\mathcal{KL}$ asymptotically stable for $\mathcal{H}_\rho := (C_\rho, F_\rho, D_\rho, G_\rho)$, the ρ-perturbation of $\mathcal{H}$. The exact definition of $\mathcal{H}_\rho$ is given in [30, Def. 6.27] and not reported here due to space constraints. The perturbed data $C_\rho \supset C$, $F_\rho \supset F$, $D_\rho \supset D$, $G_\rho \supset G$ are obtained by inflating C, F, D, G at each point $x \in \mathbb{R}^n$ by a ball whose radius is associated with the values of the positive definite function ρ at points nearby x. Since $\rho(x) > 0$ for all $x \in \mathbb{R}^n \backslash \mathcal{A}$, then $\mathcal{H}_\rho$ is a strictly larger hybrid inclusion whose data $C_\rho, F_\rho, D_\rho, G_\rho$, plugged into (1), allow for additional flowing and jumping directions. These directions generate all solutions of $\mathcal{H}$ and a funnel of perturbed solutions encoding a wide range of perturbations including unmodeled dynamics and disturbances.

In this work, we seek for a hybrid adaptive controller whose data satisfy the so-called hybrid basic conditions of [30, Assumption 6.5]. Due to [30, Thm 7.12], global asymptotic stability (GAS) of a compact set is equivalent to uniform global asymptotic stability (UGAS) and, following the robustness results in [30, §7.3], it is also equivalent to global robust $\mathcal{KL}$ asymptotic stability. UGAS and $\mathcal{KL}$ stability will be used interchangeably in the following and, by [30, Lemma 7.20], they are semiglobally practically robust to a broad range of real-world non-idealities such as measurement noise, sample-and-hold implementations [35], and actuator dynamics [38].

We refer to [30], [39] for additional definitions and tools for the analysis of hybrid systems.

II. Model Description

A. Second-Order Kuramoto Network

In this article, we consider a generalization of the celebrated Kuramoto model [1], based on the *swing equations* described in [3]. More specifically, the *second-order Kuramoto network* is a system of N nonlinear oscillators, coupled through an undirected and connected graph $\mathcal{G} = \{\mathcal{V}, \mathcal{E}\}$:

$$\begin{aligned} \dot{\theta}_i &= \omega_i, && i \in \mathcal{V} \\ m_i \dot{\omega}_i &= -d_i \omega_i + \omega_{\mathrm{n}i} + u_i - \sum_{j \in \mathcal{N}_i} k_{ij} \sin(\theta_i - \theta_j - \varphi_{ij}), \end{aligned} \tag{3}$$

where, for each $i \in \mathcal{V}$, $\theta_i \in \mathbb{R}$ and $\omega_i \in \mathbb{R}$ are the phase and the frequency, respectively, u_i is the control input, $m_i > 0$ is the oscillator's inertia, $d_i > 0$ is a damping constant, and $\omega_{\mathrm{n}i}$ is the oscillator's natural frequency. In addition, $k_{ij} = k_{ji} > 0$ and $\varphi_{ij} = \varphi_{ji} \in [0, 2\pi)$ are, respectively, the coupling weight and the phase shift between oscillators i and j. Suppose that the graph $\mathcal{G}$, associated with the physical couplings in (3), also defines the communication topology among the nodes.

Define $\theta := \begin{bmatrix} \theta_1 & \dots & \theta_N \end{bmatrix}^\top \in \mathbb{R}^N$ and $\omega := \begin{bmatrix} \omega_1 & \dots & \omega_N \end{bmatrix}^\top \in \mathbb{R}^N$, then denote by $(\theta(\cdot), \omega(\cdot)) : \mathbb{R}_{\geq 0} \to \mathbb{R}^{2N}$ a solution of system (3), for some input signals $u_i(\cdot)$, $i \in \mathcal{V}$, and with initial conditions $(\theta(0), \omega(0))$. We say that $(\theta(\cdot), \omega(\cdot))$ achieves *phase synchronization* if

$$\lim_{t \to +\infty} \theta_i(t) - \theta_j(t) \in \left\{ \tilde{\theta} : \tilde{\theta} = 2k\pi, k \in \mathbb{Z} \right\}, \quad \forall i, j \in \mathcal{V}. \tag{4}$$

Similarly, the solution $(\theta(\cdot), \omega(\cdot))$ is said to achieve *frequency synchronization* if

$$\lim_{t \to +\infty} \omega_i(t) - \omega_j(t) = 0, \qquad \forall i, j \in \mathcal{V}. \tag{5}$$

For the network (3), our objective is to design a distributed strategy that ensures robust adaptive global phase synchronization to a reference trajectory. Namely, our aim is to define feedback laws for the inputs u_i based only on local information and network communication such that, for any initialization of system (3), the corresponding solution $(\theta(\cdot), \omega(\cdot))$ achieves phase synchronization and convergence to the reference. In particular, phase synchronization is robust when, in addition to the convergence in (4), the closed-loop system admits a globally asymptotically stable compact attractor, with appropriate robustness to perturbations of the dynamics in the sense of the definitions reported in the Notation section.

Because we do not assume exact knowledge of the local parameters m_i, d_i, $\omega_{\mathrm{n}i}$, k_{ij}, and φ_{ij}, we design adaptive controllers that ensure asymptotic convergence in the presence of parametric uncertainties. At the same time, it is well known that the sensitivity of adaptive techniques to non-parametric (unmodeled) perturbations of the dynamics calls for a robust design of the adaptive law and some known bounds of the parametric uncertainty (see, e.g., [40, Chs. 8 and 9]). Accordingly, we impose the following assumption.

Assumption 1 *There exists a scalar $\varrho > 0$, known to each node $i \in \mathcal{V}$, such that:*

$$\begin{aligned} &m_i \leq \varrho, \ d_i \leq \varrho, \ |\omega_{\mathrm{n}i}| \leq \varrho, && \forall i \in \mathcal{V}, \\ &k_{ij} \leq \varrho, && \forall i \in \mathcal{V}, \forall j \in \mathcal{N}_i, \end{aligned} \tag{6}$$

where the bound ϱ is taken to be the same for all parameters for simplicity of notation.

B. Quaternion-Inspired Representation

For control design, we propose to rewrite system (3) in a more convenient form. Motivated by the equivalence modulo 2π of the phases θ_i, also reflected in the phase synchronization condition (4), we choose to represent θ_i on the unit circle $\mathbb{S}^1 := \left\{ \begin{bmatrix} \alpha & \beta \end{bmatrix}^\top \in \mathbb{R}^2 : \alpha^2 + \beta^2 = 1 \right\}$. Recall that the compact set $\mathbb{S}^1$ has Lie group structure that is isomorphic to the group of planar rotations $\mathrm{SO}(2) := \{R \in \mathbb{R}^{2\times 2} : R^\top R = I_2, \det(R) = 1\}$. In view of such an isomorphism, we define the function $\mathcal{R} : \mathbb{S}^1 \to \mathrm{SO}(2)$,

which maps any $\begin{bmatrix}\alpha & \beta\end{bmatrix}^\top \in \mathbb{S}^1$ into the corresponding rotation matrix:

$$\mathcal{R}\left(\begin{bmatrix}\alpha\\ \beta\end{bmatrix}\right) \coloneqq \begin{bmatrix}\alpha & -\beta\\ \beta & \alpha\end{bmatrix}. \tag{7}$$

Function $\mathcal{R}(\cdot)$ is useful to define the group multiplication between any $\xi, \hat{\xi} \in \mathbb{S}^1$ as $\mathcal{R}(\xi)\hat{\xi} = \mathcal{R}(\hat{\xi})\xi$ (note that $\mathbb{S}^1$ is Abelian, i.e., the group operation is commutative), where the identity element is given by $\begin{bmatrix}1\\0\end{bmatrix}$.

From the above definitions, we introduce the following representation for θ_i:

$$\zeta_i \coloneqq \begin{bmatrix}\eta_i & \epsilon_i\end{bmatrix}^\top \coloneqq \begin{bmatrix}\cos(\theta_i/2) & \sin(\theta_i/2)\end{bmatrix}^\top \in \mathbb{S}^1, \tag{8}$$

corresponding to a unit quaternion for planar rotations (cf. [27] for the parameterization adopted for 3D rotations). We refer to [36] for a detailed discussion on representation (8) and its relation with the choices in [41] and [39, Ex. 34]. Using (7) and (8), the phase dynamics on SO(2) and $\mathbb{S}^1$ is obtained as

$$\frac{d}{dt}\mathcal{R}(\zeta_i) = \frac{1}{2}\omega_i J\mathcal{R}(\zeta_i), \quad \dot{\zeta}_i = \frac{1}{2}\omega_i J\zeta_i, \qquad i \in \mathcal{V}, \tag{9}$$

where $J \coloneqq \left[\begin{smallmatrix}0 & -1\\ 1 & 0\end{smallmatrix}\right] \in \mathrm{SO}(2)$. Let $\mathbb{T}^N \coloneqq \prod_{i=1}^N \mathbb{S}^1$ denote the N-torus. The network dynamics (3) can be conveniently rewritten on $\mathbb{T}^N \times \mathbb{R}^N$ as follows:

$$\begin{aligned}\dot{\zeta}_i &= \frac{1}{2}\omega_i J\zeta_i && i \in \mathcal{V}\\ m_i\dot{\omega}_i &= -d_i\omega_i + \omega_{\mathrm{n}i} + u_i\\ &\quad -\sum_{j\in\mathcal{N}_i} k_{ij}\Big(\phi(\zeta_i)^\top J\phi(\zeta_j)\cos(\varphi_{ij}) - \phi(\zeta_i)^\top\phi(\zeta_j)\sin(\varphi_{ij})\Big)\end{aligned} \tag{10}$$

where $\phi : \mathbb{S}^1 \to \mathbb{S}^1$ is defined as

$$\phi(\zeta_i) \coloneqq \mathcal{R}(\zeta_i)\zeta_i = \begin{bmatrix}\eta_i^2 - \epsilon_i^2\\ 2\eta_i\epsilon_i\end{bmatrix}, \quad \zeta_i \coloneqq \begin{bmatrix}\eta_i\\ \epsilon_i\end{bmatrix} \tag{11}$$

and corresponds to the double angle formula from $\zeta_i \coloneqq [\cos(\theta_i/2)\ \sin(\theta_i/2)]^\top$ to $[\cos(\theta_i)\ \sin(\theta_i)]^\top$. In particular, note that model (10) is computed from (3) using (9) and the identities $\sin(\theta_i - \theta_j) = \phi(\zeta_i)^\top J\phi(\zeta_j)$, $\cos(\theta_i - \theta_j) = \phi(\zeta_i)^\top\phi(\zeta_j)$. Then, with the proposed representation (8), the condition (4) corresponding to phase synchronization becomes

$$\lim_{t\to+\infty} \mathcal{R}(\zeta_i(t))^\top\zeta_j(t) \in \left\{-\begin{bmatrix}1\\0\end{bmatrix}, \begin{bmatrix}1\\0\end{bmatrix}\right\}, \quad \forall i, j \in \mathcal{V}, \tag{12}$$

where $\mathcal{R}(\zeta_i)^\top\zeta_j = [\cos((\theta_i - \theta_j/2)\ \sin((\theta_i - \theta_j)/2)]^\top$.

Remark 1 *In some applications, such as those involving rotary encoders, θ_i is provided by sensors that "wrap" the angles in $[0, 2\pi)$ (equivalently, in $[-\pi, \pi)$). In this scenario, if (8) is used to compute ζ_i from the sensor measurement, call it θ_i^{s}, special care must be taken to ensure that a continuous trajectory of the vector $[\cos(\theta_i^{\mathrm{s}})\ \sin(\theta_i^{\mathrm{s}})]^\top$ (uniquely corresponding to any $\theta_i^{\mathrm{s}} \in [0, 2\pi)$) is mapped into a continuous trajectory of ζ_i. More specifically, for any $\theta_i^{\mathrm{s}} \in [0, 2\pi)$, there are two possible values of ζ_i, expressed through:*

$$\zeta_i \in \{-\zeta_i^*, \zeta_i^*\},$$
$$\zeta_i^* \coloneqq \begin{cases}\begin{bmatrix}\sqrt{\frac{1+\cos(\theta_i^{\mathrm{s}})}{2}} & \sqrt{\frac{1-\cos(\theta_i^{\mathrm{s}})}{2}}\end{bmatrix}^\top & \theta_i^{\mathrm{s}} \in [0, \pi)\\ \begin{bmatrix}-\sqrt{\frac{1+\cos(\theta_i^{\mathrm{s}})}{2}} & \sqrt{\frac{1-\cos(\theta_i^{\mathrm{s}})}{2}}\end{bmatrix}^\top & \theta_i^{\mathrm{s}} \in [\pi, 2\pi),\end{cases} \tag{13}$$

where $\zeta_i^* : [0, \pi) \to \mathbb{S}^1$ is a continuous function based on the half-angle formula that maps angles into elements of a half circle. The same issue arises for unit quaternions. In that context, a path-lifting mechanism has been proposed in [42] to ensure that a continuous selection of the two quaternions is obtained for a "measured" rotation matrix. For simplicity, we avoid embedding a similar mechanism as [42] by considering ζ_i available for measurement. Including the path-lifting mechanism does not affect the results of this paper.

III. Main Objective and Control Architecture

A. Leader Exosystem

Since our objective involves the synchronization of the network to a reference signal, the graph $\mathcal{G}$ is augmented with an additional node, named *leader system*, which delivers to the network some reference signals (see, e.g., [23], [41]). The references are generated through an autonomous exosystem of the form

$$\left.\begin{aligned}\dot{\zeta}^\star &= \frac{1}{2}c^\top w^\star J\zeta^\star\\ \dot{w}^\star &= s(\zeta^\star, w^\star)\end{aligned}\right\} \quad (\zeta^\star, w^\star) \in \mathcal{K}^\star \subset \mathbb{S}^1 \times \mathbb{R}^n, \tag{14}$$

where $\zeta^\star \in \mathbb{S}^1$ is the phase reference, $w^\star \in \mathbb{R}^n$, $n \in \mathbb{Z}_{\geq 1}$, is a state such that the frequency reference is given by $c^\top w^\star \in \mathbb{R}$, while $c \in \mathbb{R}^n$ is a constant vector and $s(\cdot) : \mathbb{S}^1 \times \mathbb{R}^n \to \mathbb{R}^n$ is a nonlinear function. Furthermore, $\mathcal{K}^\star$ is a compact set of admissible initial conditions $(\zeta^\star(0), w^\star(0))$.

The feedback structure in (14) suggests that, different from [22], [32], we do not restrict the structure of exosystem (14) to a cascade between the $w^\star$-subsystem and the $\zeta^\star$-subsystem. We remark that the data of exosystem (14) are not related to the structure of the open-loop Kuramoto dynamics (10). Instead, we only require the following properties for (14).

Assumption 2 *For system (14), it holds that:*

1) *the compact set $\mathcal{K}^\star$ is forward invariant;*
2) *the map $s(\cdot)$ is globally Lipschitz, with Lipschitz constant $\ell_s \geq 0$;*
3) *c and $s(\cdot)$ are known to each node $i \in \mathcal{V}$.*

The global Lipschitz condition in Assumption 2 is instrumental in achieving global asymptotic stability, cf. [43]. As we shall see in Section IV, this Lipschitz continuity property allows designing the controllers for each node $i \in \mathcal{V}$ without

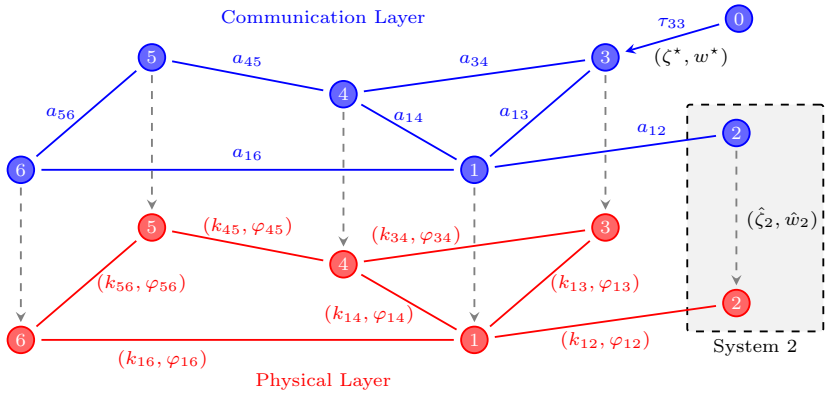

Fig. 1. Interaction and communication scheme. The same graph will be employed for the numerical example in Section VII.

the explicit knowledge of the compact set $\mathcal{K}^\star$. As remarked in [43], global Lipschitz continuity is a mild assumption because it merely requires a reasonable incremental behavior of the nonlinear dynamics. For example, for any locally Lipschitz continuous $s(\cdot)$, this property can be easily obtained by artificially modifying the function outside the domain of interest $\mathcal{K}^\star$. As a final requirement for our design, we impose a standard assumption describing the communication topology among the leader (14) and the network (10).

Assumption 3 *System* (14) *interacts, by communicating the reference* $(\zeta^\star, w^\star)$*, with at least one node of graph* $\mathcal{G}$*, which defines both the physical couplings and the communication topology. In other words,* $\mathcal{T} \neq \emptyset$ *(equivalently,* $T \neq 0$*).*

Remark 2 *Since* $\mathcal{G}$ *is undirected and connected, Assumption 3 implies that the leader-follower matrix* $B := L + T$ *is positive definite, where* L *is the Laplacian matrix and* T *is the target matrix, cf. the Notation subsection related to graph theory.*

Fig. 1 shows a scheme of the physical and communication layers underlying our distributed architecture.

B. Problem Statement and Control Architecture

The control problem of this work can be stated as follows.

Problem 1 *Under Assumptions 1, 2, and 3, design a distributed adaptive strategy, only based on the local measurements* (ζ_i, ω_i) *and the information exchange according to graph* $\mathcal{G}$*, such that the second-order Kuramoto network* (10) *achieves robust adaptive global phase synchronization to the leader exosystem, involving global phase synchronization as in* (12) *and convergence to* $\zeta^\star$*:*

$$\lim_{t\to+\infty} \mathcal{R}(\zeta_i(t))^\top \zeta^\star \in \left\{ -\begin{bmatrix}1\\0\end{bmatrix}, \begin{bmatrix}1\\0\end{bmatrix} \right\}, \quad \forall i \in \mathcal{V}. \tag{15}$$

In addition to solving the above synchronization problem, our control solution will be shown to globally asymptotically stabilize a suitable compact set, thereby enjoying the intrinsic robustness properties induced by well-posed hybrid dynamics as discussed in the Notation subsection.

We represent in Fig. 2 the architecture of our distributed controller solving Problem 1, which also serves as a summary for the contents of the next Sections IV, V. From Fig. 2 one can clearly see the effect of the two-layer network structure of Fig. 1, where the physical layer (in red) only affects the oscillators dynamics, whereas the communication layer (in blue) is used to exchange information among neighboring control nodes. Each control node $i \in \mathcal{V}$ comprises the next components, well represented in Fig. 2.

- A *distributed observer* for exosystem (14), whose developments are given in Section IV, ensuring global asymptotic estimation of $(\zeta^\star, w^\star) \in \mathcal{K}^\star$ via local estimates $(\hat{\zeta}_i, \hat{w}_i)$ of $(\zeta^\star, w^\star) \in \mathcal{K}^\star$, defined as elements of $\mathbb{R}^{2+n}$, that allow obtaining global results despite the generality of the exosystem dynamics (as stated in Assumption 2 relaxing the previous requirements in [22], [32]) and of the graph topology (as stated in Assumption 3 not imposing acyclic graphs and relaxing typical requirements [21]). The ensuing estimation error dynamics are described by two feedback-interconnected subsystems, associated with the phase and the frequency estimation errors, respectively. These subsystems are proven to be ISS and then combined through small-gain arguments.
- A *hybrid synchronizer* (developed in Section V-A) of the local oscillator phase ζ_i with the estimate $\hat{\zeta}_i$ provided by

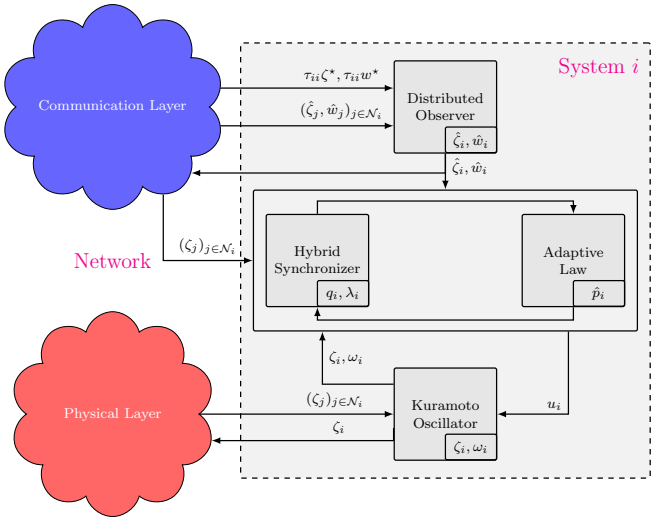

Fig. 2. Control architecture and interconnection with the network.

the observer. The hybrid mechanism ensures $\mathcal{R}(\zeta_i)^\top \hat{\zeta}_i \to \left\{ -\begin{bmatrix}1\\0\end{bmatrix}, \begin{bmatrix}1\\0\end{bmatrix} \right\}$, $\omega_i \to c^\top \hat{w}_i$. The design is performed by initially supposing that ω_i can be assigned as a virtual input ω_{vi}, so that a hybrid hysteresis-based mechanism (overcoming intrinsic limitations of continuous feedback laws) ensures both global phase synchronization together with the useful property that the virtual input ω_{vi} is constant across jumps (a contribution of independent interest about hybrid synchronization on $\mathbb{S}^1$).

- A *backstepping-based adaptive law* (developed in Section V-B) designed to adapt to the unknown dynamics of the local oscillators whose parametric uncertainties satisfy Assumption 1. The adaptive law guarantees that the frequency ω_i synchronizes with the virtual input ω_{vi} commanded by the hybrid synchronizer.

In the remainder of the paper, after a detailed characterization of the three above-described components (estimator, synchronizer, adaptation) in Sections IV and V, we summarize the overall control scheme in Section VI, where we also state our main result.

IV. Distributed Observer

In order to solve Problem 1, we propose the following distributed observer:

$$\begin{aligned} \dot{\hat{\zeta}}_i &= \frac{1}{2} c^\top \hat{w}_i J \hat{\zeta}_i - k_\zeta e_{\zeta i} \\ \dot{\hat{w}}_i &= s(\hat{\zeta}_i, \hat{w}_i) - k_w e_{w_i} \end{aligned} \qquad i \in \mathcal{V}, \tag{16}$$

where $\hat{\zeta}_i \in \mathbb{R}^2$ and $\hat{w}_i \in \mathbb{R}^n$ are, respectively, the estimates at node i of $\zeta^\star \in \mathbb{S}^1$ and $w^\star \in \mathbb{R}^n$ of (14), k_ζ and $k_w \in \mathbb{R}$ are gains to be designed, while

$$\begin{aligned} e_{\zeta i} &:= \sum_{j \in \mathcal{N}_i} (\hat{\zeta}_i - \hat{\zeta}_j) + \tau_{ii}(\hat{\zeta}_i - \zeta^\star) \\ e_{w_i} &:= \sum_{j \in \mathcal{N}_i} (\hat{w}_i - \hat{w}_j) + \tau_{ii}(\hat{w}_i - w^\star) \end{aligned} \qquad i \in \mathcal{V}, \tag{17}$$

are the *local estimation errors*, and τ_{ii} are the diagonal entries of the target matrix T defined in the Notation subsection.

Observer (16) is distributed as it is only driven by locally available quantities (17). To represent the variables for the overall network in a compact form, it is convenient to use the Kronecker product. In particular, define the overall states $\hat{\zeta} := [\hat{\zeta}_1^\top \ \dots \ \hat{\zeta}_N^\top]^\top \in \mathbb{R}^{2N}$ and $\hat{w} := [\hat{w}_1^\top \ \dots \ \hat{w}_N^\top]^\top \in \mathbb{R}^{Nn}$, so that the overall estimation errors are $\tilde{\zeta} := \hat{\zeta} - \mathbf{1}_N \otimes \zeta^\star$ and $\tilde{w} := \hat{w} - \mathbf{1}_N \otimes w^\star$. Furthermore, define $e_\zeta := [e_{\zeta_1}^\top \ \dots \ e_{\zeta_N}^\top]^\top \in \mathbb{R}^{2N}$ and $e_w := [e_{w_1}^\top \ \dots \ e_{w_N}^\top]^\top \in \mathbb{R}^{Nn}$, which from (17) can be written as [44]:

$$e_\zeta = (B \otimes I_2)\tilde{\zeta}, \qquad e_w = (B \otimes I_n)\tilde{w}, \tag{18}$$

where the leader-follower matrix $B := L + T$ satisfies $B = B^\top > 0$ as discussed in Remark 2. We recall that $\underline{\sigma}(B) > 0$ denotes the smallest singular value of matrix B.

A. Phase Subnetwork

We start by analyzing the $(\zeta^\star, \hat{\zeta})$-subsystem (referred to as phase subnetwork) and the phase estimation error $\tilde{\zeta}$. From (14), (16), the phase subnetwork obeys dynamics

$$\begin{aligned} \dot{\zeta}^\star &= \frac{1}{2} c^\top w^\star J \zeta^\star \\ \dot{\hat{\zeta}}_i &= \frac{1}{2} c^\top w^\star J \hat{\zeta}_i + \frac{1}{2} c^\top \tilde{w}_i J \hat{\zeta}_i - k_\zeta e_{\zeta i}, \quad i \in \mathcal{V}. \end{aligned} \tag{19}$$

For notational convenience, define

$$\tilde{\Omega} := \operatorname{diag}(c^\top \tilde{w}_1, \dots, c^\top \tilde{w}_N) = \operatorname{diag}((I_N \otimes c^\top)\tilde{w}), \tag{20}$$

which allows writing the dynamics of $\hat{\zeta}$ in compact form as follows

$$\dot{\hat{\zeta}} = \frac{1}{2}\left(c^\top w^\star (I_N \otimes J) + (\tilde{\Omega} \otimes J) \right) \hat{\zeta} - k_\zeta e_\zeta. \tag{21}$$

As a consequence, the dynamics of the phase estimation error $\tilde{\zeta} := \hat{\zeta} - \mathbf{1}_N \otimes \zeta^\star$, can be computed from (18), (19), (21) as:

$$\begin{aligned} \dot{\tilde{\zeta}} = &\left(\frac{1}{2} c^\top w^\star (I_N \otimes J) - k_\zeta (B \otimes I_2) + \frac{1}{2}(\tilde{\Omega} \otimes J) \right) \tilde{\zeta} \\ &+ \frac{1}{2}(\tilde{\Omega} \otimes J)(\mathbf{1}_N \otimes \zeta^\star), \end{aligned} \tag{22}$$

with inputs given by $\zeta^\star$, $w^\star$, and $\tilde{w}$ (through $\tilde{\Omega}$ in (20)). The next proposition provides an ISS characterization for (22).

Proposition 1 *For any scalar gain $k_\zeta > 0$, system (22) is finite-gain exponentially input-to-state stable with respect to the input $\tilde{w}$, uniformly in the inputs $(\zeta^\star, w^\star)$. Namely, for any solution $(\zeta^\star(\cdot), w^\star(\cdot))$ of the exosystem (14) and any $\tilde{w}(\cdot) \in \mathcal{L}_\infty$, the solutions of (22) satisfy, for all $t \geq 0$:*

$$|\tilde{\zeta}(t)| \leq \max\left\{ \mathrm{e}^{-\frac{1}{2}\underline{\sigma}(B)k_\zeta t}|\tilde{\zeta}(0)|, \frac{|c|\|\tilde{w}(\cdot)\|_\infty}{\underline{\sigma}(B)k_\zeta} \right\}. \tag{23}$$

Proof: For any solution $(\zeta^\star(\cdot), w^\star(\cdot))$ of exosystem (14), system (22) can be regarded as a time-varying system with input $\tilde{w}$. It is convenient to rewrite the last term of (22) as

$$\begin{aligned} (\tilde{\Omega} \otimes J)(\mathbf{1}_N \otimes \zeta^\star) &= \tilde{\Omega}\mathbf{1}_N \otimes J\zeta^\star \\ &= \operatorname{diag}((I_N \otimes c^\top)\tilde{w})\mathbf{1}_N \otimes J\zeta^\star \\ &= \operatorname{diag}(\mathbf{1}_N)(I_N \otimes c^\top)\tilde{w} \otimes J\zeta^\star \\ &= \underbrace{(I_N \otimes J\zeta^\star c^\top)}_{:=Z^\star}\tilde{w} = Z^\star \tilde{w}, \end{aligned} \tag{24}$$

where we used the identity $((I_N \otimes c^\top)w) \otimes v = (I_N \otimes vc^\top)w$, which holds for any vectors $c^\top$, w, v, of compatible dimensions. Consider the Lyapunov function candidate

$$V_\zeta := \frac{1}{2}|\tilde{\zeta}|^2 \tag{25}$$

whose derivative along the trajectories of (22) results in

$$\begin{aligned} \dot{V}_\zeta = &-k_\zeta \tilde{\zeta}^\top (B \otimes I_2)\tilde{\zeta} + \frac{1}{2}\tilde{\zeta}^\top Z^\star \tilde{w} \\ &+ \frac{1}{2}\tilde{\zeta}^\top \left(c^\top w^\star (I_N \otimes J) + (\tilde{\Omega} \otimes J) \right) \tilde{\zeta}, \\ = &-k_\zeta \tilde{\zeta}^\top (B \otimes I_2)\tilde{\zeta} + \frac{1}{2}\tilde{\zeta}^\top Z^\star \tilde{w}, \end{aligned} \tag{26}$$

where we employed the fact that $I_N \otimes J$ and $\tilde{\Omega} \otimes J$ are skew symmetric. Since $k_\zeta > 0$, we obtain

$$\dot{V}_\zeta \leq -\underline{\sigma}(B) k_\zeta |\tilde{\zeta}|^2 + \frac{1}{2}|Z^\star||\tilde{\zeta}||\tilde{w}|. \tag{27}$$

The following computations yield $|Z^\star| = |c|$:

$$\begin{aligned} |Z^\star| &= |I_N||J\zeta^\star c^\top| = |J\zeta^\star c^\top| \\ &= |J\zeta^\star c^\top|_F = \sqrt{\mathrm{Tr}(c\zeta^{\star\top} J^\top J \zeta^\star c^\top)} \\ &= \sqrt{\mathrm{Tr}(cc^\top)} = |c|, \end{aligned} \tag{28}$$

where $|J\zeta^\star c^\top| = |J\zeta^\star c^\top|_F$ since the rank of $J\zeta^\star c^\top$ is 1 by construction. Applying (27) and (28) yields

$$|\tilde{\zeta}| \geq \frac{|c|}{\underline{\sigma}(B)k_\zeta}|\tilde{w}| \implies \dot{V}_\zeta \leq -\frac{\underline{\sigma}(B)k_\zeta}{2}|\tilde{\zeta}|^2, \tag{29}$$

which leads to (23) via standard ISS calculations [33, Thm. 10.4.1]. □

B. Frequency Subnetwork

Starting again from (14), (16), the frequency subnetwork obeys dynamics

$$\begin{aligned} \dot{w}^\star &= s(\zeta^\star, w^\star) \\ \dot{\hat{w}}_i &= s(\hat{\zeta}_i, \hat{w}_i) - k_w e_{w_i}, \quad i \in \mathcal{V}. \end{aligned} \tag{30}$$

We can then write the dynamics of $\hat{w}$ as

$$\dot{\hat{w}} = S(\hat{\zeta}, \hat{w}) - k_w e_w, \tag{31}$$

where

$$S(\hat{\zeta}, \hat{w}) := \begin{bmatrix} s(\hat{\zeta}_1, \hat{w}_1) \\ \vdots \\ s(\hat{\zeta}_N, \hat{w}_N) \end{bmatrix}. \tag{32}$$

Therefore, using (18), the dynamics of the frequency estimation error $\tilde{w} := \hat{w} - (\mathbf{1}_N \otimes w^\star)$ is given by

$$\dot{\tilde{w}} = S(\hat{\zeta}, \hat{w}) - \mathbf{1}_N \otimes s(\zeta^\star, w^\star) - k_w(B \otimes I_n)\tilde{w}, \tag{33}$$

which, in view of $\hat{\zeta} = \tilde{\zeta} + \mathbf{1}_N \otimes \zeta^\star$, $\hat{w} = \tilde{w} + \mathbf{1}_N \otimes w^\star$, is a non-autonomous system with inputs given by $\zeta^\star$, $w^\star$, and $\tilde{\zeta}$. In the following, we present a result that follows the same structure as Proposition 1, now applied to the frequency subnetwork.

Proposition 2 *For any scalar gain $k_w > \ell_s/\underline{\sigma}(B)$, system (33) is finite-gain exponentially input-to-state stable with respect to the input $\tilde{\zeta}$, uniformly in the inputs $(\zeta^\star, w^\star)$. Namely, for any solution $(\zeta^\star(\cdot), w^\star(\cdot))$ of the exosystem (14) and any $\tilde{\zeta}(\cdot) \in \mathcal{L}_\infty$, the solutions of system (33) satisfy, for all $t \geq 0$:*

$$|\tilde{w}(t)| \leq \max\left\{ \mathrm{e}^{-\frac{1}{2}(\underline{\sigma}(B)k_w - \ell_s)t}|\tilde{w}(0)|, \frac{2\ell_s \|\tilde{\zeta}(\cdot)\|_\infty}{\underline{\sigma}(B)k_w - \ell_s} \right\}. \tag{34}$$

Proof: For any solution $(\zeta^\star(\cdot), w^\star(\cdot))$ of the exosystem (14), system (33) can be regarded as a time-varying system with input $\tilde{\zeta}$. Consider the Lyapunov function candidate

$$V_w := \frac{1}{2}|\tilde{w}|^2, \tag{35}$$

whose derivative along the trajectories of (33) is

$$\begin{aligned} \dot{V}_w &= -k_w \tilde{w}^\top (B \otimes I_n)\tilde{w} + \tilde{w}^\top \left(S(\hat{\zeta}, \hat{w}) - \mathbf{1}_N \otimes s(\zeta^\star, w^\star) \right) \\ &= -k_w \tilde{w}^\top (B \otimes I_n)\tilde{w} + \sum_{i=1}^N \tilde{w}_i^\top \left(s(\hat{\zeta}_i, \hat{w}_i) - s(\zeta^\star, w^\star) \right). \end{aligned} \tag{36}$$

By Assumption 2, it holds that

$$|s(\hat{\zeta}_i, \hat{w}_i) - s(\zeta^\star, w^\star)| \leq \ell_s(|\tilde{\zeta}_i| + |\tilde{w}_i|), \tag{37}$$

therefore we conclude that

$$\begin{aligned} \dot{V}_w &\leq -\underline{\sigma}(B)k_w|\tilde{w}|^2 + \ell_s \sum_{i=1}^N \left(|\tilde{w}_i|^2 + |\tilde{w}_i||\tilde{\zeta}_i| \right) \\ &\leq -\left(\underline{\sigma}(B)k_w - \ell_s \right)|\tilde{w}|^2 + \ell_s |\tilde{w}||\tilde{\zeta}|. \end{aligned} \tag{38}$$

From (38) we obtain the following ISS characterization:

$$|\tilde{w}| \geq \frac{2\ell_s}{\underline{\sigma}(B)k_w - \ell_s}|\tilde{\zeta}| \implies \dot{V}_w \leq -\frac{\underline{\sigma}(B)k_w - \ell_s}{2}|\tilde{w}|^2, \tag{39}$$

which proves the finite-gain exponential ISS bound (34) through [33, Thm. 10.4.1]. □

C. Overall Observer Analysis

We conclude the section with a stability result for the feedback interconnection between the phase estimation error dynamics (22) and the frequency estimation error dynamics (33).

Theorem 1 *For any choice of the scalar gains k_ζ and k_w such that*

$$\begin{aligned} &k_\zeta > 0, \qquad k_w > \ell_s/\underline{\sigma}(B), \\ &k_\zeta \underline{\sigma}(B)(k_w \underline{\sigma}(B) - \ell_s) - 2\ell_s|c| > 0, \end{aligned} \tag{40}$$

the zero-equilibrium $(\tilde{\zeta}, \tilde{w}) = 0$ of the overall estimation error system (22), (33) is globally exponentially stable.

Proof: From Proposition 1, which holds for $k_\zeta > 0$, and Proposition 2, valid for $k_w\underline{\sigma}(B) > \ell_s$, we obtain that both (22) and (33) are finite-gain exponentially ISS. Therefore, global exponential stability is ensured from (23), (34), and [33, Thm. 10.6.1], through the following small-gain condition:

$$\frac{2\ell_s|c|}{k_\zeta \underline{\sigma}(B)(k_w\underline{\sigma}(B) - \ell_s)} < 1, \tag{41}$$

which is ensured by (40). □

We stress that small-gain arguments are essential to treat the potential richness of the nonlinearities at the right-hand side of the $w^\star$-dynamics of exosystem (14). We also emphasize that our approach does not impose any requirement

on the frequency dynamics of the underlying Kuramoto model (10), which is completely handled by the adaptive mechanism described in the next section and represented in Fig. 2. Due to the generality of our assumptions, as discussed in the following remark, our design ensures higher flexibility with respect to other observers proposed in the literature.

Remark 3 *In the special case where exosystem* (14) *is a cascade, i.e., $s = s(w^\star)$, conditions* (40) *collapse to $k_\zeta > 0$, $k_w > \ell_s/\underline{\sigma}(B)$. Additionally, if $s(w^\star) = S_w w^\star$, where S_w is a Poisson stable matrix as in [22], [32], [36],* (36) *becomes $\dot{V}_w = -k_w \tilde{w}^\top (B \otimes I_n)\tilde{w}$, so that conditions* (40) *collapse to $k_\zeta > 0$, $k_w > 0$.*

V. Synchronization with Global Knowledge of the Leader Signals

In this section, we design a tracking controller for the simplified setup where the observer estimation errors are zero. This approach will be motivated in Section VI by the reduction arguments of the stability analysis.

Firstly, we compute the local tracking error dynamics. Define the phase and frequency tracking errors as

$$\begin{aligned} \bar{\zeta}_i &\coloneqq \begin{bmatrix} \bar{\eta}_i & \bar{\epsilon}_i \end{bmatrix}^\top \coloneqq \mathcal{R}(\zeta_i)^\top \hat{\zeta}_i \in \mathbb{R}^2 \\ \bar{\omega}_i &\coloneqq c^\top \hat{w}_i - \omega_i \in \mathbb{R} \end{aligned} \qquad i \in \mathcal{V}. \tag{42}$$

In these coordinates, the control objective in Problem 1 corresponds to imposing $\bar{\epsilon}_i \to 0$, for all $i \in \mathcal{V}$. From (10), (16), and $\mathcal{R}(\zeta_i)^\top J = J\mathcal{R}(\zeta_i)^\top$, we can compute the phase error dynamics as

$$\begin{aligned} \dot{\bar{\zeta}}_i &= \frac{d}{dt}\left(\mathcal{R}(\zeta_i)^\top\right)\hat{\zeta}_i + \mathcal{R}(\zeta_i)^\top \dot{\hat{\zeta}}_i \\ &= -\mathcal{R}(\zeta_i)^\top \frac{d\mathcal{R}(\zeta_i)}{dt}\mathcal{R}(\zeta_i)^\top \hat{\zeta}_i + \mathcal{R}(\zeta_i)^\top \dot{\hat{\zeta}}_i \quad i \in \mathcal{V} \\ &= \frac{1}{2}\bar{\omega}_i J \bar{\zeta}_i - k_\zeta \mathcal{R}(\zeta_i)^\top e_{\zeta_i}. \end{aligned} \tag{43}$$

Similarly, the dynamics of the frequency error $\bar{\omega}_i$ is computed from (10), (14), and (16) as

$$m_i \dot{\bar{\omega}}_i = \psi_i - u_i - m_i k_w c^\top e_{w_i}, \qquad i \in \mathcal{V}, \tag{44}$$

where we defined

$$\begin{aligned} \psi_i \coloneqq\ & m_i c^\top s(\hat{\zeta}_i, \hat{w}_i) + d_i \omega_i - \omega_{\mathrm{n}i} \\ & + \sum_{j \in \mathcal{N}_i} k_{ij} \phi(\zeta_i)^\top J \phi(\zeta_j) \cos(\varphi_{ij}) \\ & - \sum_{j \in \mathcal{N}_i} k_{ij} \phi(\zeta_i)^\top \phi(\zeta_j) \sin(\varphi_{ij}). \end{aligned} \tag{45}$$

Observe that, with $\hat{\zeta}_i = \zeta^\star$ and $\hat{w}_i = w^\star$ (i.e., $\tilde{\zeta} = 0$, $\tilde{w} = 0$, equivalently, $e_\zeta = 0$, $e_w = 0$), the quantities in (42) become $\bar{\zeta}_i = \mathcal{R}(\zeta_i)^\top \zeta^\star \in \mathbb{S}^1$ and $\bar{\omega}_i = c^\top w^\star - \omega_i \in \mathbb{R}$. In view of this reduction argument, we begin the design by assuming that the exosystem signals $(\zeta^\star, w^\star)$ are globally known for feedback. This scenario corresponds to the requirement $\mathcal{T} = \mathcal{V}$, which will be removed in Section VI.

A. Phase Synchronization

Assume initially that ω_i can be arbitrarily assigned by the feedback controller as a virtual input $\omega_{\mathrm{v}i}$. With $e_\zeta = 0$, the dynamics (43) thus reduces to

$$\dot{\bar{\zeta}}_i = \frac{1}{2}(c^\top \hat{w}_i - \omega_{\mathrm{v}i}) J \bar{\zeta}_i, \qquad i \in \mathcal{V}, \tag{46}$$

where $\omega_{\mathrm{v}i}$ is the virtual input that should ensure $\bar{\epsilon}_i \to 0$. We refer to this objective as *phase synchronization* with the reference $\zeta^\star$.

Define $\mathcal{Q} \coloneqq \{-1, 1\}$ and choose any gain $k > 0$ and a hysteresis margin $\delta \in (0, 1)$. For each $i \in \mathcal{V}$, a hysteresis-based hybrid dynamic controller that achieves global phase synchronization is given by

$$\begin{aligned} &\begin{cases} \dot{q}_i = 0, & (\bar{\zeta}_i, q_i) \in C_\kappa \\ q_i^+ = -q_i, & (\bar{\zeta}_i, q_i) \in D_\kappa \end{cases} \qquad i \in \mathcal{V} \\ &\omega_{\mathrm{v}i} = c^\top \hat{w}_i + k q_i \bar{\epsilon}_i, \end{aligned} \tag{47}$$

where $q_i \in \mathcal{Q}$ is the controller state and[1]

$$\begin{aligned} C_\kappa &\coloneqq \{(\bar{\zeta}_i, q_i) \in \mathbb{S}^1 \times \mathcal{Q} : \bar{\eta}_i q_i \geq -\delta\} \\ D_\kappa &\coloneqq \{(\bar{\zeta}_i, q_i) \in \mathbb{S}^1 \times \mathcal{Q} : \bar{\eta}_i q_i \leq -\delta\}. \end{aligned} \tag{48}$$

The closed-loop error dynamics then corresponds to

$$\begin{cases} \dot{\bar{\zeta}}_i = -\frac{1}{2} k q_i \bar{\epsilon}_i J \bar{\zeta}_i \\ \dot{q}_i = 0, \end{cases} \begin{bmatrix} \bar{\zeta}_i \\ q_i \end{bmatrix} \in C_\kappa, \quad \begin{cases} \bar{\zeta}_i^+ = \bar{\zeta}_i \\ q_i^+ = -q_i, \end{cases} \begin{bmatrix} \bar{\zeta}_i \\ q_i \end{bmatrix} \in D_\kappa, \tag{49}$$

which provides an autonomous hybrid dynamics having state $(\bar{\zeta}_i, q_i) = ((\bar{\eta}_i, \bar{\epsilon}_i), q_i) \in \mathbb{S}^1 \times \mathcal{Q}$ and such that $q_i \bar{\eta}_i = -1$ is not included in the flow set C_κ (because $\delta < 1$). The next lemma is a straightforward derivation from [27].

Lemma 1 *For any $k > 0$ and $\delta \in (0, 1)$, the attractor $\mathcal{A}_\kappa \coloneqq \left\{(\bar{\zeta}_i, q_i) \in \mathbb{S}^1 \times \mathcal{Q} : \bar{\zeta}_i = q_i \begin{bmatrix} 1 \\ 0 \end{bmatrix}\right\}$ is UGAS for the hybrid system* (49).

Proof: Choose the Lyapunov function

$$V_\kappa(\bar{\zeta}_i, q_i) \coloneqq 2(1 - q_i \bar{\eta}_i), \tag{50}$$

which is positive definite and radially unbounded with respect to $\mathcal{A}_\kappa$. Denoting $\dot{V}_\kappa = \left\langle \nabla V_\kappa, [\dot{\bar{\zeta}}_i \ \dot{q}_i]^\top \right\rangle$ and $\Delta V_\kappa = V_\kappa(\bar{\zeta}_i^+, q_i^+) - V_\kappa(\bar{\zeta}_i, q_i)$, straightforward calculations yield

$$\begin{aligned} \dot{V}_\kappa &= -k\bar{\epsilon}_i^2 < 0, \qquad \forall (\bar{\zeta}_i, q_i) \in C_\kappa \backslash \mathcal{A}_\kappa \\ \Delta V_\kappa &= 4 q_i \bar{\eta}_i \leq -4\delta < 0, \quad \forall (\bar{\zeta}_i, q_i) \in D_\kappa, \end{aligned} \tag{51}$$

implying UGAS from standard hybrid Lyapunov theory. □

For a convenient design of the backstepping-based adaptive controller defined in the next subsection, we propose now a dynamically extended version of (47) to ensure that $\omega_{\mathrm{v}i}$

[1] We employ the subscript i in (48) to indicate the variables of a generic node i of the graph. The same convention is adopted throughout this section, cf. $\mathcal{A}_\kappa$ in Lemma 1, and (53).

remains constant across jumps. Specifically, we augment the controller with a first-order filter of the feedback $kq_i\bar{\epsilon}_i$:

$$\begin{cases} \dot{q}_i = 0 \\ \dot{\lambda}_i = -h(\lambda_i - kq_i\bar{\epsilon}_i) & (\bar{\zeta}_i, q_i, \lambda_i) \in C_\lambda \\ \end{cases} \quad i \in \mathcal{V}, \\ \begin{cases} q_i^+ = -q_i \\ \lambda_i^+ = \lambda_i \end{cases} \quad (\bar{\zeta}_i, q_i, \lambda_i) \in D_\lambda \tag{52}$$

where h is a positive gain and the sets C_λ, D_λ are defined as the next generalization of (48):

$$C_\lambda := \left\{ (\bar{\zeta}_i, q_i, \lambda_i) \in \mathbb{S}^1 \times \mathcal{Q} \times \mathbb{R} : \left(\bar{\eta}_i + \frac{\lambda_i \bar{\epsilon}_i}{k} \right) q_i \geq -\delta \right\}$$
$$D_\lambda := \left\{ (\bar{\zeta}_i, q_i, \lambda_i) \in \mathbb{S}^1 \times \mathcal{Q} \times \mathbb{R} : \left(\bar{\eta}_i + \frac{\lambda_i \bar{\epsilon}_i}{k} \right) q_i \leq -\delta \right\}. \tag{53}$$

We can then replace by λ_i the term $kq_i\bar{\epsilon}_i$ in the selection of $\omega_{\mathrm{v}i}$ of (47), namely we choose:

$$\omega_{\mathrm{v}i} = c^\top \hat{w}_i + \lambda_i, \qquad i \in \mathcal{V}, \tag{54}$$

which remains constant across jumps. The closed-loop error dynamics for each node i, obtained from the interconnection of (46), (52), and (54), is described by:

$$\begin{cases} \dot{\bar{\zeta}}_i = -\frac{1}{2}\lambda_i J \bar{\zeta}_i \\ \dot{q}_i = 0 \\ \dot{\lambda}_i = -h(\lambda_i - kq_i\bar{\epsilon}_i) \end{cases} \begin{bmatrix} \bar{\zeta}_i \\ q_i \\ \lambda_i \end{bmatrix} \in C_\lambda, \quad \begin{cases} \bar{\zeta}_i^+ = \bar{\zeta}_i \\ q_i^+ = -q_i \\ \lambda_i^+ = \lambda_i \end{cases} \begin{bmatrix} \bar{\zeta}_i \\ q_i \\ \lambda_i \end{bmatrix} \in D_\lambda. \tag{55}$$

The next result generalizes the argument of Lemma 1.

Proposition 3 *For any $k > 0$, $\delta \in (0,1)$, and $h > k$, the attractor $\mathcal{A}_\lambda := \left\{ (\bar{\zeta}_i, q_i, \lambda_i) \in \mathbb{S}^1 \times \mathcal{Q} \times \mathbb{R} : \bar{\zeta}_i = q_i \begin{bmatrix} 1 \\ 0 \end{bmatrix}, \lambda_i = 0 \right\}$ is UGAS for the hybrid system* (55).

Proof: Define $\tilde{\lambda}_i := \lambda_i - kq_i\bar{\epsilon}_i$, then consider the Lyapunov function

$$V_\lambda(\bar{\zeta}_i, q_i, \lambda_i) := 2k^2(1 - q_i\bar{\eta}_i) + \tilde{\lambda}_i^2. \tag{56}$$

Note that V_λ is positive definite with respect to $\mathcal{A}_\lambda$ and radially unbounded relative to $\mathbb{S}^1 \times \mathcal{Q} \times \mathbb{R}$. Denote $\dot{V}_\lambda = \left\langle \nabla V_\lambda, [\dot{\bar{\zeta}}_i \ \dot{q}_i \ \dot{\lambda}_i]^\top \right\rangle$. For all $(\bar{\zeta}_i, q_i, \lambda_i) \in C_\lambda$, it holds that

$$\begin{aligned} \dot{V}_\lambda &= -k^2 q_i \lambda_i \bar{\epsilon}_i + \tilde{\lambda}_i(-2h\tilde{\lambda}_i + kq_i\lambda_i\bar{\eta}_i) \\ &= -k^3\bar{\epsilon}_i^2 + k^2\tilde{\lambda}_i\bar{\epsilon}_i(\bar{\eta}_i - q_i) - (2h - kq_i\bar{\eta}_i)\tilde{\lambda}_i^2 \\ &\leq -\begin{bmatrix} |\bar{\epsilon}_i| \\ |\tilde{\lambda}_i| \end{bmatrix}^\top \underbrace{\begin{bmatrix} k^3 & -k^2 \\ -k^2 & 2h-k \end{bmatrix}}_{M} \begin{bmatrix} |\bar{\epsilon}_i| \\ |\tilde{\lambda}_i| \end{bmatrix}. \end{aligned} \tag{57}$$

From $\delta < 1$, for any point in C_λ we have that $\tilde{\lambda}_i = 0$ and $\bar{\epsilon}_i = 0$ implies $(\bar{\zeta}_i, q_i, \lambda_i) \in \mathcal{A}$ (in particular, the point with $\lambda_i = 0$ and $q_i = -\bar{\eta}_i$ does not belong to C_λ), then $\dot{V}_\lambda < 0$, for all $(\bar{\zeta}_i, q_i, \lambda_i) \in C_\lambda \backslash \mathcal{A}_\lambda$, if $k^3(2h-k) - k^4 = 2k^3(h-k) > 0$, i.e., $h > k$. On the other hand, denote $\Delta V_\lambda = V_\lambda(\bar{\zeta}_i^+, q_i^+, \lambda_i^+) - V_\kappa(\bar{\zeta}_i, q_i, \lambda_i)$, then for all $(\bar{\zeta}_i, q_i, \lambda_i) \in D_\lambda$ we have:

$$\begin{aligned} \Delta V_\lambda &= 4k^2 q_i \bar{\eta}_i + (\tilde{\lambda}_i + 2kq_i\bar{\epsilon}_i)^2 - \tilde{\lambda}_i^2 \\ &= 4k^2 q_i \left(\bar{\eta}_i + \frac{\lambda_i \bar{\epsilon}_i}{k} \right) \leq -4k^2\delta < 0, \end{aligned} \tag{58}$$

thus concluding UGAS for the attractor $\mathcal{A}_\lambda$. □

B. Global Adaptive Synchronization

Taking advantage of the hybrid system defined in (52), we propose to achieve global synchronization to the reference $\zeta^\star$ using an adaptive backstepping controller where, in place of the feedback $\omega_{\mathrm{v}i} = c^\top \hat{w}_i + \lambda_i$ in (54), we ensure $\omega_i \to \omega_{\mathrm{v}i}$ by design of the control input u_i.

In place of the frequency tracking error $\bar{\omega}_i$ in (42), consider the error variable

$$z_i := c^\top \hat{w}_i + \lambda_i - \omega_i = \bar{\omega}_i + \lambda_i \in \mathbb{R}, \qquad i \in \mathcal{V}. \tag{59}$$

We can rewrite the error dynamics (43) and (44) using variables z_i as follows:

$$\begin{aligned} \dot{\bar{\zeta}}_i &= \frac{1}{2}(z_i - \lambda_i) J \bar{\zeta}_i - k_\zeta \mathcal{R}(\zeta_i)^\top e_{\zeta i} \\ m_i \dot{z}_i &= \psi_i - u_i - m_i \left(k_w c^\top e_{w_i} + h(\lambda_i - kq_i\bar{\epsilon}_i) \right) \end{aligned} \quad i \in \mathcal{V}. \tag{60}$$

Using (45), the second equation can be rewritten as follows

$$m_i \dot{z}_i = \Psi_i^\top p_i - u_i - m_i k_w c^\top e_{w_i}, \qquad i \in \mathcal{V}, \tag{61}$$

with regressor Ψ_i and parameter vector $p_i \in \mathbb{R}^{3+2|\mathcal{N}_i|}$ given by:

$$\Psi_i := \begin{bmatrix} c^\top s(\hat{\zeta}_i, \hat{w}_i) - h(\lambda_i - kq_i\bar{\epsilon}_i) \\ \omega_i \\ 1 \\ \phi(\zeta_i)^\top J \phi(\zeta_{j_1}) \\ \vdots \\ \phi(\zeta_i)^\top J \phi(\zeta_{j_{|\mathcal{N}_i|}}) \\ \phi(\zeta_i)^\top \phi(\zeta_{j_1}) \\ \vdots \\ \phi(\zeta_i)^\top \phi(\zeta_{j_{|\mathcal{N}_i|}}) \end{bmatrix}, \ p_i := \begin{bmatrix} m_i \\ d_i \\ -\omega_{\mathrm{n}i} \\ k_{ij_1} \cos(\varphi_{ij_1}) \\ \vdots \\ k_{ij_{N_i}} \cos(\varphi_{ij_{|\mathcal{N}_i|}}) \\ -k_{ij_1} \sin(\varphi_{ij_1}) \\ \vdots \\ -k_{ij_{N_i}} \sin(\varphi_{ij_{|\mathcal{N}_i|}}) \end{bmatrix} \tag{62}$$

where we denoted $\mathcal{N}_i = \{j_1, \ldots, j_{|\mathcal{N}_i|}\}$. By Assumption 1, it follows that

$$|p_i|_\infty = \max\{|p_{i1}|, \ldots, |p_{i(3+2|\mathcal{N}_i|)}|\} \leq \varrho. \tag{63}$$

The control of system (60) is based on the augmentation of control law (52) with the following adaptive state-input selections:

$$\begin{aligned} u_i &= \Psi_i^\top \hat{p}_i + k_z z_i \\ \dot{\hat{p}}_i &= \gamma \Psi_i z_i - \gamma\nu \, \mathrm{dz}(\hat{p}_i) \qquad i \in \mathcal{V}, \\ \hat{p}_i^+ &= \hat{p}_i, \end{aligned} \tag{64}$$

where k_z, γ, and ν are positive gains, while $\mathrm{dz}:\mathbb{R}^{3+2|\mathcal{N}_i|}\to\mathbb{R}^{3+2|\mathcal{N}_i|}$ is a component-wise dead-zone function defined as [45, §3.4]:

$$\mathrm{dz}(\xi) \coloneqq \begin{bmatrix} \xi_1 - \varrho\mathrm{sat}\left(\frac{\xi_1}{\varrho}\right) \\ \vdots \\ \xi_{3+2|\mathcal{N}_i|} - \varrho\mathrm{sat}\left(\frac{\xi_{3+2|\mathcal{N}_i|}}{\varrho}\right) \end{bmatrix}, \tag{65}$$

where $\mathrm{sat}(y) \coloneqq \max\{-1,\min\{1,y\}\}$. Exploiting (63), it can be verified that, for all p_i and all $\xi\in\mathbb{R}^{3+2|\mathcal{N}_i|}$:

$$(\xi - p_i)^\top \mathrm{dz}(\xi) \geq 0. \tag{66}$$

Moreover, there exist positive scalars r and μ such that, for all p_i and all $\xi\in\mathbb{R}^{3+2|\mathcal{N}_i|}$:

$$|\xi|\geq r \implies (\xi-p_i)^\top \mathrm{dz}(\xi)\geq \mu|\xi|^2. \tag{67}$$

In view of our reduction arguments ($e_{\zeta_i}=0$ and $e_{w_i}=0$ in (60)), the closed-loop system obtained from the interconnection of the phase/frequency tracking error dynamics (60), (61), the first-order filter (52), and the adaptive controller (64), having state $x_i\coloneqq(\bar\zeta_i,q_i,\lambda_i,z_i,\hat p_i)$, is expressed, for each $i\in\mathcal{V}$, as follows:

$$\begin{cases} \dot{\bar\zeta}_i = \frac{1}{2}(z_i-\lambda_i)J\bar\zeta_i \\ \dot q_i = 0 \\ \dot\lambda_i = -h(\lambda_i - kq_i\bar\epsilon_i) \\ m_i\dot z_i = -k_z z_i - \Psi_i^\top(\hat p_i - p_i) \\ \dot{\hat p}_i = \gamma\Psi_i z_i - \gamma\nu\,\mathrm{dz}(\hat p_i) \end{cases} \quad x_i\in C_i, \quad \begin{cases} \bar\zeta_i^+ = \bar\zeta_i \\ q_i^+ = -q_i \\ \lambda_i^+ = \lambda_i \\ z_i^+ = z_i \\ \hat p_i^+ = \hat p_i \end{cases} \quad x_i\in D_i, \tag{68}$$

where $C_i\coloneqq C_\lambda\times\mathbb{R}^{4+2|\mathcal{N}_i|}$ and $D_i\coloneqq C_z\times\mathbb{R}^{4+2|\mathcal{N}_i|}$. In the following, we focus on the stability properties of the closed-loop system obtained through the interconnection of the exosystem (14) and the local error dynamics (68). For this interconnection, we are going to show that there exists a globally asymptotically stable compact attractor $\mathcal{A}_0$ and, in addition, that all oscillators are synchronized with the reference $\zeta^\star$. More specifically, global phase synchronization corresponds to global attractivity of the set $\mathcal{K}_0$, defined as:

$$\begin{aligned}\mathcal{K}_0 \coloneqq \{(\zeta^\star,w^\star,x_1,\dots,x_N)\in\mathcal{K}^\star\times\prod_{i\in\mathcal{V}}(\mathbb{S}^1\times\mathcal{Q}\times\mathbb{R}^{5+2|\mathcal{N}_i|}):\\ \bar\zeta_i = q_i\begin{bmatrix}1\\0\end{bmatrix}, \lambda_i=0, z_i=0, |\hat p_i|\leq r, \forall i\in\mathcal{V}\},\end{aligned} \tag{69}$$

where $r>0$ as per (67). In the sequel, we call $\mathcal{K}_0$ *synchronization set*.

Remark 4 *The set $\mathcal{K}_0$ is compact. Indeed, $(\zeta^\star,w^\star)\in\mathcal{K}^\star$ is in a compact by assumption, while the only possibly unbounded components of $x_i\coloneqq(\bar\zeta_i,q_i,\lambda_i,z_i,\hat p_i)$ are λ_i, z_i, and $\hat p_i$. Therefore, from the conditions in* (69)*, compactness follows immediately.*

Remark 5 *Since no persistency of excitation is necessarily satisfied by the regressor Ψ_i in* (62)*, it might be surprising that a globally asymptotically stable attractor can be found with the considered adaptive controller. This result is possible because we make use of the analysis tools in [30, Ch. 6.10] instead of the standard tools for adaptive control (see, e.g., [46, §8.3]). In particular, we leverage the result [30, Cor. 7.7], which states that, under some regularity properties including-well posedness, the ω-limit set from a compact set of initial conditions is locally asymptotically stable.*

Theorem 2 *For any selection of the tuning parameters $k>0$, $\delta\in(0,1)$, $h>k$, $k_z>0$, $\gamma>0$, and $\nu>0$, the following properties hold for the interconnection of the exosystem* (14) *and the local tracking error dynamics* (68)*:*

1) *there exists a robustly globally $\mathcal{KL}$ asymptotically stable compact attractor $\mathcal{A}_0$;*
2) *the synchronization set $\mathcal{K}_0$ in* (69) *is globally attractive. In particular, all solutions achieve global phase synchronization as per* (15)*.*

Proof: First, we prove that the closed-loop solutions are bounded and forward complete. Then, we prove the two items. The state $(\zeta^\star,w^\star)$ of the exosystem (14) evolves in the bounded forward invariant set $\mathcal{K}^\star$, thus it is bounded. Define:

$$W_i(z_i,\hat p_i)\coloneqq\frac{1}{2}m_i z_i^2 + \frac{1}{2\gamma}|\hat p_i - p_i|^2, \qquad \forall i\in\mathcal{V}. \tag{70}$$

Along the closed-loop solutions, we obtain from (68),

$$\begin{aligned}\dot W_i &= -k_z z_i^2 - z_i\Psi_i^\top(\hat p_i - p_i) + (\hat p_i - p_i)^\top\left[\Psi_i z_i - \nu\,\mathrm{dz}(\hat p_i)\right] \\ &= -k_z z_i^2 - \nu(\hat p_i - p_i)^\top\mathrm{dz}(\hat p_i), \qquad \forall i\in\mathcal{V}.\end{aligned} \tag{71}$$

Boundedness of x_i, $i\in\mathcal{V}$, is established by using the following Lyapunov function

$$V_i(x_i)\coloneqq V_\lambda(\bar\zeta_i,q_i,\lambda_i) + gW_i(z_i,\hat p_i), \tag{72}$$

where $g>0$ is a positive scalar and V_λ is given in (56). From (57), (68), (71), and choosing $g=k^4/(\underline{\sigma}(M)k_z)$ we obtain, for all $i\in\mathcal{V}$:

$$\begin{aligned}\dot V_i &\leq -\underline{\sigma}(M)(\bar\epsilon_i^2+\tilde\lambda_i^2) + k^2 q_i\bar\epsilon_i z_i + g\dot W_i \\ &\leq -\underline{\sigma}(M)(\bar\epsilon_i^2+\tilde\lambda_i^2) + \frac{\underline{\sigma}(M)}{2}\bar\epsilon_i^2 + \frac{gk_z}{2}z_i^2 + g\dot W_i \\ &\leq -\frac{\underline{\sigma}(M)}{2}(\bar\epsilon_i^2+2\tilde\lambda_i^2) - \frac{gk_z}{2}z_i^2 - g\nu(\hat p_i - p_i)^\top\mathrm{dz}(\hat p_i).\end{aligned} \tag{73}$$

Therefore, using (67) and the properties of the dead-zone function, we conclude that, for all $i\in\mathcal{V}$,

$$\begin{aligned}\dot V_i &\leq -\tfrac{\underline{\sigma}(M)}{2}(\bar\epsilon_i^2+2\tilde\lambda_i^2) - \tfrac{gk_z}{2}z_i^2 \leq 0, && \text{if } |\hat p_i|\leq r, \\ \dot V_i &\leq -\tfrac{\underline{\sigma}(M)}{2}(\bar\epsilon_i^2+2\tilde\lambda_i^2) - \tfrac{gk_z}{2}z_i^2 - \nu\mu|\hat p_i|^2 < 0, && \text{if } |\hat p_i|\geq r.\end{aligned} \tag{74}$$

Finally, from (58) and the fact that z_i and $\hat p_i$ do not change across jumps in (68), it holds that

$$\Delta V_i \leq -4k^2\delta < 0, \qquad \forall i\in\mathcal{V}. \tag{75}$$

Properties (74) and (75) show forward invariance of the sublevel sets of V_i, $i\in\mathcal{V}$, thus x_i is contained in a compact

set, for all $i \in \mathcal{V}$. From the boundedness of x_i, $i \in \mathcal{V}$, we conclude by [30, Prop. 6.10] that the solutions are forward complete, thus they are precompact.

Next, we show item 1 of the statement. For all $i \in \mathcal{V}$, pick sublevel sets Γ_i of V_i such that $\dot{V}_i < 0$ for all $x_i \in C_i \cap \partial\Gamma_i$, and note that this set is globally attractive. Define the set $\Gamma \coloneqq \prod_{i\in\mathcal{V}} \Gamma_i$. For a set of initial conditions of the form $\Gamma_\varepsilon \coloneqq \Gamma + \varepsilon\mathbb{B}$ where $\varepsilon > 0$ is an arbitrary scalar and $\mathbb{B}$ is a closed unit ball, it holds that $\mathcal{A}_0 \coloneqq \Omega(\Gamma_\varepsilon) \subset \Gamma \subset \mathrm{Int}(\Gamma_\varepsilon)$, where $\Omega(\Gamma_\varepsilon)$ denotes the ω-limit set of Γ_ε. By [30, Cor. 7.7], $\mathcal{A}_0$ is asymptotically stable (therefore Lyapunov stable) with basin of attraction containing Γ_ε. From the previous arguments, $\mathcal{A}_0$ is globally attractive, which, together with its Lyapunov stability, gives GAS. Since the hybrid dynamics satisfies the hybrid basic conditions of [30, As. 6.5] and $\mathcal{A}_0$ is compact, then GAS of $\mathcal{A}_0$ implies robust global $\mathcal{KL}$ asymptotic stability from [30, Thm. 7.21].

Finally, from (74), (75), we apply [30, Cor. 8.4] to obtain that all solutions approach the largest weakly invariant subset of $\mathcal{K}_0$, thus proving item 2 of the statement. □

As customary in adaptive control, convergence of the estimated parameters $\hat{p}_i$ to the true parameters p_i cannot be guaranteed.

Additionally, we remark that it is difficult, if at all possible, to give an explicit representation of the attractor $\mathcal{A}_0$. Even without an explicit representation, the mere existence of $\mathcal{A}_0$ is sufficient to ensure in the next section a uniform global asymptotic stability result for the overall closed-loop system.

VI. Main Result

We finally present the complete hybrid observer-based controller for each node i, obtained by combining the distributed observer (16), the local hysteresis-based controller (52), and the local adaptive controller (64). Note that, in this context, we no longer assume $\tilde{\zeta} = 0$, $\tilde{w} = 0$ (equivalently, $e_\zeta = 0$, $e_w = 0$), thus the dynamics of the tracking errors $(\tilde{\zeta}_i, z_i)$ in (60) is not simplified as in the scenario with known leader signals. The robustness property established in Theorem 2 is naturally inherited here due to well posedness of the hybrid dynamics, which allows for a range of relevant real-world perturbed scenarios as discussed in the Notation.

Define the overall state at node i as

$$\chi_i \coloneqq (\hat{\zeta}_i, \hat{w}_i, \underbrace{\bar{\zeta}_i, q_i, \lambda_i, z_i, \hat{p}_i}_{x_i}) \in \mathbb{R}^{n+4}\times\mathcal{Q}\times\mathbb{R}^{5+2|\mathcal{N}_i|}, \quad (76)$$

then the local controllers that solve Problem 1 are given as follows, for each $i \in \mathcal{V}$:

$$\begin{cases} \dot{\hat{\zeta}}_i = \dfrac{1}{2}c^\top \hat{w}_i J \hat{\zeta}_i - k_\zeta e_{\zeta i} \\ \dot{\hat{w}}_i = s(\hat{\zeta}_i, \hat{w}_i) - k_w e_{w_i} \\ \dot{q}_i = 0 \\ \dot{\lambda}_i = -h(\lambda_i - k q_i \bar{\epsilon}_i) \\ \dot{\hat{p}}_i = \gamma \Psi_i z_i - \gamma\nu\,\mathrm{dz}(\hat{p}_i) \end{cases} \chi_i \in C_{\chi i}, \quad \begin{cases} \hat{\zeta}_i^+ = \hat{\zeta}_i \\ \hat{w}_i^+ = \hat{w}_i \\ q_i^+ = -q_i \\ \lambda_i^+ = \lambda_i \\ \hat{p}_i^+ = \hat{p}_i \end{cases} \chi_i \in D_{\chi i},$$

$$\text{with: } C_{\chi i} \coloneqq \left\{ \chi_i \in \mathbb{R}^{n+4} \times \mathcal{Q} \times \mathbb{R}^{5+2|\mathcal{N}_i|} : \left(\bar{\eta}_i + \frac{\lambda_i \bar{\epsilon}_i}{k}\right) q_i \geq -\delta \right\},$$

$$D_{\chi i} \coloneqq \left\{ \chi_i \in \mathbb{R}^{n+4} \times \mathcal{Q} \times \mathbb{R}^{5+2|\mathcal{N}_i|} : \left(\bar{\eta}_i + \frac{\lambda_i \bar{\epsilon}_i}{k}\right) q_i \leq -\delta \right\},$$

$$\text{and:} \quad u_i = \Psi_i^\top \hat{p}_i + k_z z_i, \quad (77)$$

where the local estimation errors $e_{\zeta i}$, e_{w_i} are given in (17), the components $\bar{\eta}_i$, $\bar{\epsilon}_i$ of the phase tracking error $\bar{\zeta}_i$ are defined in (42), the frequency tracking error z_i is defined in (59), regressor Ψ_i is given in (62), the dead-zone function dz is given in (65), while the tuning parameters are the observer gains k_ζ, k_w, the synchronizer gains k, h, k_z, δ, and the adaptive law gains γ, ν.

The closed-loop system is given by the interconnection of the second-order Kuramoto network (10), the exosytem (14), and the local controllers (77). For such system, we exploit reduction theorems to show that there exists a compact attractor $\mathcal{A}$ that is robustly globally $\mathcal{KL}$ asymptotically stable. Furthermore, as for Theorem 2, we show that the compact set:

$$\mathcal{K} \coloneqq \{(\zeta^\star, w^\star, \chi_1, \ldots, \chi_N) \in \mathcal{K}^\star \times \prod_{i\in\mathcal{V}} (\mathbb{R}^{n+4} \times \mathcal{Q} \times \mathbb{R}^{5+2|\mathcal{N}_i|}) : \hat{\zeta}_i = \zeta^\star, \hat{w}_i = w^\star, \bar{\zeta}_i = q_i \begin{bmatrix} 1 \\ 0 \end{bmatrix}, \lambda_i = z_i = 0, |\hat{p}_i| \leq r, \forall i \in \mathcal{V}\}, \quad (78)$$

is globally attractive. Similar to (69), we call $\mathcal{K}$ *synchronization set* because its elements enjoy phase synchronization to the reference $\zeta^\star$. Note that the projection of $\mathcal{K}$ in the direction of $(\zeta^\star, w^\star, x_1, \ldots, x_N)$ corresponds to $\mathcal{K}_0$ in (69).

The main result of this work is given by the following statement, which provides formal guarantees for the effectiveness of the controllers (77).

Theorem 3 *For any selection of the tuning parameters $k > 0$, $\delta \in (0, 1)$, $h > k$, $k_z > 0$, $\gamma > 0$, $\nu > 0$ and k_ζ, k_w satisfying* (40)*, the following properties hold for the interconnection among the second-order Kuramoto model* (10)*, the leader exosystem* (14)*, and the local controllers* (77)*:*

1) *there exists a robustly globally $\mathcal{KL}$ asymptotically stable compact attractor $\mathcal{A}$;*

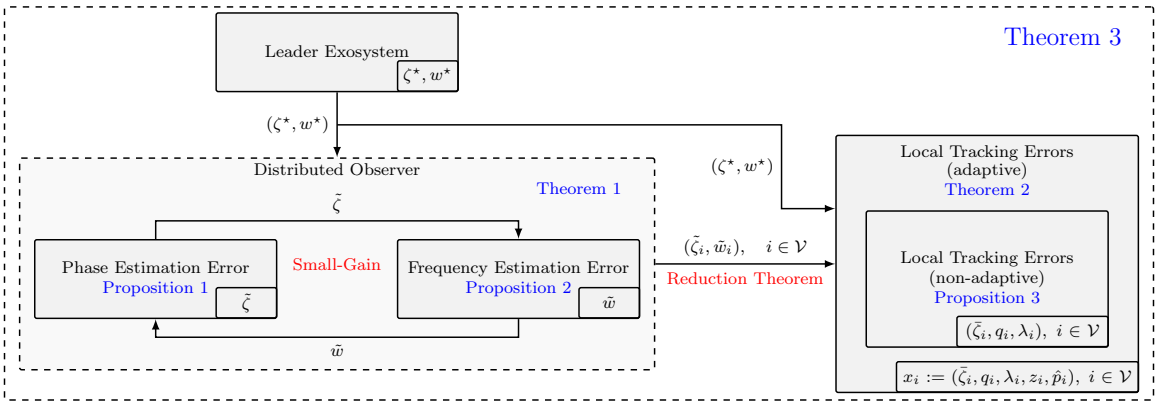

Fig. 3. Sketch of the closed-loop error subsystems, with their interconnections and the related stability results.

2) *the synchronization set $\mathcal{K}$ in* (78) *is globally attractive. In particular, all solutions achieve global phase synchronization as per* (15)*, thus solving Problem 1.*

Proof: We begin by highlighting the cascade structure of the closed-loop error dynamics. As shown in Section IV, the distributed observer dynamics are collected in the estimation error subsystems (22), (33). We can establish a cascade interconnection between system (22), (33), (14), with output $(\zeta^\star, w^\star, \tilde\zeta, \tilde w)$, and the tracking error dynamics (68). Note that when $(\tilde\zeta, \tilde w) = 0$ the closed-loop system is described by the dynamics with known leader signals (14), (68). The interconnection of these subsystems is shown in Fig. 3.

Asymptotic stability of the attractor $\mathcal{A}$ is proven through reduction theorems. By Theorem 1, we showed that the closed (but not compact) attractor

$$\hat{\mathcal{A}} := \{(\zeta^\star, w^\star, \chi_1, \dots, \chi_N) \in \mathcal{K}^\star \times \prod_{i\in\mathcal{V}} (\mathbb{R}^{n+4} \times \mathcal{Q} \times \mathbb{R}^{5+2|\mathcal{N}_i|}) : \hat\zeta_i = \zeta^\star, \hat w_i = w^\star, \forall i \in \mathcal{V}\}, \tag{79}$$

corresponding to the scenario with known leader signals, is UGAS. On the set $\hat{\mathcal{A}}$, we recover the dynamics (68), thus by Theorem 2 there exists an attractor $\mathcal{A}$ that is UGAS relative to $\hat{\mathcal{A}}$. By [31, Cor 4.8], $\mathcal{A}$ is uniformly asymptotically stable for the overall closed-loop system, with basin of attraction given by all the initial conditions generating bounded solutions.

Next, we show that all solutions of the closed-loop system are bounded, which then implies UGAS of $\mathcal{A}$. First note that the state $(\zeta^\star, w^\star)$ of the exosystem (14) evolves in the bounded forward invariant set $\mathcal{K}^\star$. Similarly, q_i is bounded by construction. Due to Theorem 1, $(\tilde\zeta, \tilde w)$ converge to zero, therefore $(\hat\zeta_i, \hat w_i)$ are bounded for all $i \in \mathcal{V}$. It remains to show that $\bar\zeta_i$, λ_i, z_i, and $\hat p_i$ are bounded, for all $i \in \mathcal{V}$. Concerning $\bar\zeta_i$, recall that $\bar\zeta_i := \mathcal{R}(\zeta_i)^\top \hat\zeta_i$, where $\zeta_i \in \mathbb{S}^1$, therefore $\bar\zeta_i$ is bounded because $|\bar\zeta_i| \le |\hat\zeta_i|$. Since $\bar\zeta_i$ is bounded, so is $kq_i\bar\epsilon_i$. Then, from $|kq_i\bar\epsilon_i| \le \bar k_i$ we obtain, for $|\lambda_i| \ge \bar k_i$:

$$\begin{aligned}\frac{d}{dt}|\lambda_i| &= -h\frac{\lambda_i}{|\lambda_i|}(\lambda_i - kq_i\bar\epsilon_i) \\ &\le -h(|\lambda_i| - \bar k_i) \le 0,\end{aligned} \qquad i \in \mathcal{V}, \tag{80}$$

therefore, λ_i is bounded. To analyze $(z_i, \hat p_i)$, consider the Lyapunov function

$$W_i(z_i, \hat p_i) := \frac{1}{2} m_i z_i^2 + \frac{1}{2\gamma}|\hat p_i - p_i|^2, \qquad i \in \mathcal{V}. \tag{81}$$

From (66) and (67), respectively for each $i \in \mathcal{V}$, similar steps to those in the proof of Theorem 2 yield:

$$\begin{aligned}\dot W_i &= -k_z z_i^2 - \nu(\hat p_i - p_i)^\top \mathrm{dz}(\hat p_i) - m_i k_w z_i c^\top e_{w_i} \\ &\le -\frac{k_z}{2} z_i^2 + \frac{1}{2k_z}|m_i k_w c^\top e_{w_i}|^2, \\ |\hat p_i| \ge r \implies \dot W_i &\le -\frac{k_z}{2} z_i^2 - \nu\mu|\hat p_i|^2 + \frac{1}{2k_z}|m_i k_w c^\top e_{w_i}|^2\end{aligned} \tag{82}$$

These two bounds provide, respectively,

$$\begin{aligned}|z_i| > \frac{m_i k_w |c|}{k_z}|e_{w_i}| &\implies \dot W_i(z_i, \hat p_i) < 0, \\ |\hat p_i| > \max\left\{r, \frac{m_i k_w |c|}{\sqrt{2k_z\nu\mu}}|e_{w_i}|\right\} &\implies \dot W_i(z_i, \hat p_i) < 0.\end{aligned} \tag{83}$$

The two implications above prove that neither z_i nor $\hat p_i$ can grow unbounded because $e_w = (B \otimes I_n)\tilde w$ is bounded. Therefore, we conclude global boundedness of solutions. Noticing that the closed-loop system satisfies the hybrid basic conditions (see [30, §6.2]), thus [30, Thm. 7.21] ensures robust global $\mathcal{KL}$ asymptotic stability of $\mathcal{A}$.

Finally, we focus on attractivity of the synchronization set $\mathcal{K}$ in (78). In Theorem 1, we have proven global exponential stability of the zero-equilibrium $(\tilde\zeta, \tilde w) = 0$ of system (22), (33). Here, we additionally show that $V_{\mathrm{obs}}(\tilde\zeta, \tilde w) := V_\lambda(\tilde\zeta) + V_w(\tilde w)$, with V_λ and V_w given in (35), (25), is a Lyapunov function for (22), (33). Indeed, from (26), (38), and the gain conditions (40), straightforward computations show that

$$\dot V_{\mathrm{obs}} \le -\frac{\underline\sigma(B)k_\zeta}{2}|\tilde\zeta|^2 - \frac{\underline\sigma(B)k_w - \ell_s}{2}|\tilde w|^2. \tag{84}$$

Now define

$$V \coloneqq \sum_{i=1}^{N} W_i(z_i, \hat{p}_i) + gV_{\text{obs}}, \tag{85}$$

with $g > 0$. From $|e_w| \leq |B||\tilde{w}|$, (82), and standard arguments for continuous-time cascaded systems, it is possible to choose $g > 0$ sufficiently large so that $\dot{V} \leq -\sum_{i=1}^{N} k_z z_i^2/2 - g_1 V_{\text{obs}}$, for some $g_1 > 0$. Therefore, due to precompactness of solutions and the above inequality on $\dot{V}$, we can apply to V the hybrid invariance principle in [30, Cor. 8.4] to prove that all solutions approach the largest weakly invariant subset of $\hat{\mathcal{A}}$ in (79) also satisfying $z_i = 0$, for all $i \in \mathcal{V}$. Finally, the solutions restricted to such set satisfy $\dot{\hat{p}}_i = 0$, $|\hat{p}_i| \leq r$, and (55), for all $i \in \mathcal{V}$, thus UGAS of $\mathcal{A}_\lambda$ in Proposition 3 ensures global attractivity of $\mathcal{K}$ in (78). □

VII. Numerical Example

For the numerical analysis, we consider a Kuramoto model composed of six oscillators, whose parameters and initial conditions are reported in Tab. I. In particular, the graph of the network is depicted in Fig. 1, where the coupling parameters have been assigned as $k_{12} = 0.5$, $k_{13} = 3$, $k_{14} = 1$, $k_{16} = 1.5$, $k_{34} = 2$, $k_{45} = 2.5$, $k_{56} = 2$, $\varphi_{12} = \pi/2$, $\varphi_{13} = \pi/3$, $\varphi_{14} = \pi/4$, $\varphi_{16} = \pi/3$, $\varphi_{34} = \pi/5$, $\varphi_{45} = \pi/4$, $\varphi_{56} = \pi/2$. We suppose to have a rough knowledge of the parameter bounds by letting $\varrho = 25$ in (6). It follows that Assumptions 1 and 3 hold. The leader exosystem (14) has been chosen as

$$\begin{aligned} \frac{d}{dt}\begin{bmatrix}\zeta_1^\star \\ \zeta_2^\star\end{bmatrix} &= \frac{1}{2}(w_1^\star + w_3^\star) J \begin{bmatrix}\zeta_1^\star \\ \zeta_2^\star\end{bmatrix} \\ \frac{d}{dt}\begin{bmatrix}w_1^\star \\ w_2^\star \\ w_3^\star\end{bmatrix} &= \begin{bmatrix} 0 \\ w_3^\star \\ -w_2^\star + \left(1 - \frac{1}{2}|w_3^\star|\right)\tanh(w_3^\star) + \frac{3}{2}\zeta_2^\star \end{bmatrix}, \end{aligned} \tag{86}$$

with initial conditions $\zeta^\star(0) = [1\ 0]^\top$ and $w^\star(0) = [2\ 0\ 0]^\top$. For completeness, we briefly prove that Assumption 2 is satisfied. The existence of $\mathcal{K}^\star$ is guaranteed by proving boundedness of solutions of (86). Note that $(\zeta_1^\star, \zeta_2^\star, w_1^\star)$ are bounded by construction. On the other hand, boundedness of $(w_2^\star, w_3^\star)$ is proven by direct application of [47, Thm. 2]. We remark that, from the chosen initial conditions, the solution converges to a periodic orbit as depicted in Figs. 4, 5. It can be easily shown that $s(\hat{\zeta}^\star, w^\star)$ is globally Lipschitz, since the derivative of the nonlinear term is bounded for all $w_3^\star$. From the numerical evaluation of the differential of s over the values of $(\zeta^\star, w^\star)$, we established a Lipschitz constant $\ell_s = 2.129$.

The Kuramoto model has been implemented according to (3), with the angles θ_i wrapped between -2π and 2π in order to ensure boundedness of the simulation variables. Then, for the computation of the feedback laws, the variables ζ_i have been computed according to (8). The tuning parameters have been selected as $k_\zeta = 50$, $k_w = 50$, $\delta = 0.5$, $k = 1$, $k_z = 5$, $h = 2$, $\gamma = 1$, $\nu = 1$. Note that (40) is verified since $\underline{\sigma}(B) = 0.1136$. The initial conditions for controller (77) have been randomly chosen, where in particular the logic variables q_i have been initialized in the set $\mathcal{Q} \coloneqq \{-1, 1\}$.

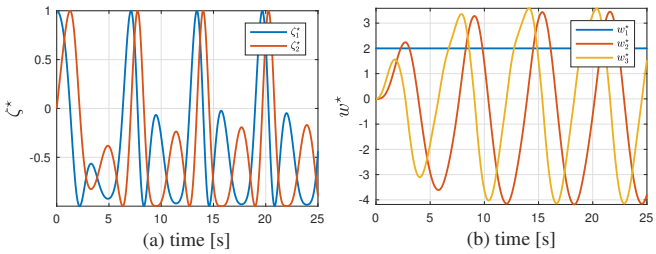

Fig. 4. Response of exosystem (86) initialized in $\boldsymbol{\zeta^\star(0) = [1\ 0]^\top}$, $\boldsymbol{w^\star(0) = [2\ 0\ 0]^\top}$.

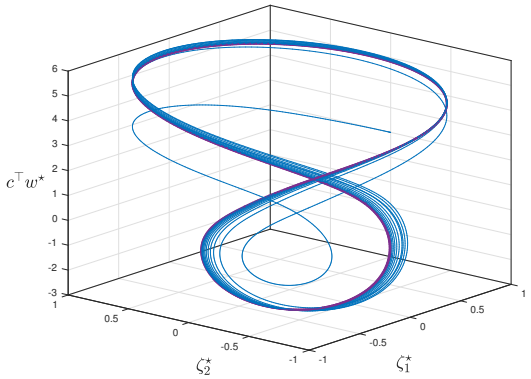

Fig. 5. Response of exosystem (86) (in blue) and corresponding asymptotic behavior (in violet).

TABLE I
Parameters and initial conditions of the oscillators

	m_i	d_i	$\omega_{\text{n}i}$	$\theta_i(0)$	$\omega_i(0)$
oscillator #1	1.1	0.1	5	$-\pi$	2
oscillator #2	1.3	0.15	10	π	0.5
oscillator #3	1.2	0.2	15	$\pi/2$	1
oscillator #4	1.6	0.21	20	$-\pi/2$	0.3
oscillator #5	1.4	0.18	8	$\pi/3$	1.5
oscillator #6	1.5	0.13	18	$-\pi/3$	0.8

In Figs. 6, 7 we report the results of a simulation run. Fig. 6 shows the behavior of the distributed observer, which rapidly converges to the exosystem signals. On the other hand, Fig. 7 depicts the tracking performance. In Fig. 7-(e), we also report the evolution of $\hat{p}_1$, showing that the parameters of the adaptive controllers converge to constant values. Finally, we employ wrapped angles to depict the phase tracking performance in Figs. 7-(f), 7-(g). In particular, we define

$$\begin{aligned} \vartheta^\star &\coloneqq \text{mod}\left(2\text{atan2}\left(\zeta_2^\star, \zeta_1^\star\right) + \pi, 2\pi\right) - \pi, \\ \vartheta_i &\coloneqq \text{mod}\left(\theta_i + \pi, 2\pi\right) - \pi, \qquad i \in \mathcal{V}, \end{aligned} \tag{87}$$

where $\vartheta^\star$ is the angular reference corresponding to $\zeta^\star$, while ϑ_i is θ_i wrapped in the interval $[-\pi, \pi)$.

VIII. Conclusions

We introduced a hybrid control strategy for the robust adaptive global phase synchronization of second-order Ku-

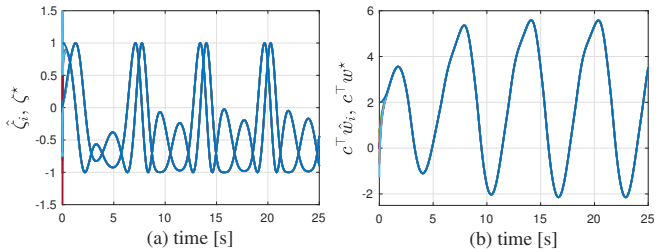

Fig. 6. Closed-loop simulation results. (a): distributed observer phase estimation (reference in blue); (b): distributed observer frequency estimation (reference in blue).

ramoto oscillators. The objective of phase synchronization was cast into a leader-follower tracking problem, where the leader system is modeled as an autonomous nonlinear exosystem. Under fairly mild assumptions on the network topology and the exosystem dynamics, we proved that our design, which comprises a distributed observer and an adaptive hybrid stabilizer, ensures the existence of a robustly globally $\mathcal{KL}$ asymptotically stable compact set for the closed-loop system and global phase synchronization. In particular, robust adaptive stabilization was ensured without requiring persistency of excitation conditions. Future efforts will be dedicated to relaxing the information requirements (e.g., by removing the frequency measurements) and the connectivity properties of the network. Furthermore, it will be worth generalizing the approach to a broader class of nonlinear oscillators.

REFERENCES

[1] Y. Kuramoto, *Chemical Oscillations, Waves, and Turbulence*. Springer, 1984.

[2] Y. Guo, D. Zhang, Z. Li, Q. Wang, and D. Yu, "Overviews on the applications of the Kuramoto model in modern power system analysis," *International Journal of Electrical Power & Energy Systems*, vol. 129, p. 106804, 2021.

[3] F. Dörfler and F. Bullo, "Synchronization and transient stability in power networks and nonuniform Kuramoto oscillators," *SIAM Journal on Control and Optimization*, vol. 50, no. 3, pp. 1616–1642, 2012.

[4] T. Menara, G. Baggio, D. S. Bassett, and F. Pasqualetti, "A framework to control functional connectivity in the human brain," in *2019 IEEE 58th Conference on Decision and Control (CDC)*. IEEE, 2019, pp. 4697–4704.

[5] Y. Qin, Y. Kawano, O. Portoles, and M. Cao, "Partial phase cohesiveness in networks of networks of Kuramoto oscillators," *IEEE Transactions on Automatic Control*, 2021.

[6] Y.-P. Choi, S.-Y. Ha, and S.-B. Yun, "Complete synchronization of Kuramoto oscillators with finite inertia," *Physica D: Nonlinear Phenomena*, vol. 240, no. 1, pp. 32 – 44, 2011.

[7] L. Wu and H. Chen, "Synchronization conditions for a third-order Kuramoto network," in *2020 59th IEEE Conference on Decision and Control (CDC)*. IEEE, 2020, pp. 5834–5839.

[8] S.-Y. Ha, M. Kang, and D. Kim, "Emergent behaviors of high-dimensional Kuramoto models on Stiefel manifolds," *Automatica*, vol. 136, no. 110072, 2022.

[9] J. Markdahl, D. Proverbio, and J. Goncalves, "Robust synchronization of heterogeneous robot swarms on the sphere," in *2020 59th IEEE Conference on Decision and Control (CDC)*. IEEE, 2020, pp. 5798–5803.

[10] S.-Y. Ha, T. Ha, and J.-H. Kim, "On the complete synchronization of the Kuramoto phase model," *Physica D: Nonlinear Phenomena*, vol. 239, no. 17, pp. 1692 – 1700, 2010.

[11] Y. Zhang and R. Xiao, "Synchronization of Kuramoto oscillators in small-world networks," *Physica A: Statistical Mechanics and its Applications*, vol. 416, pp. 33 – 40, 2014.

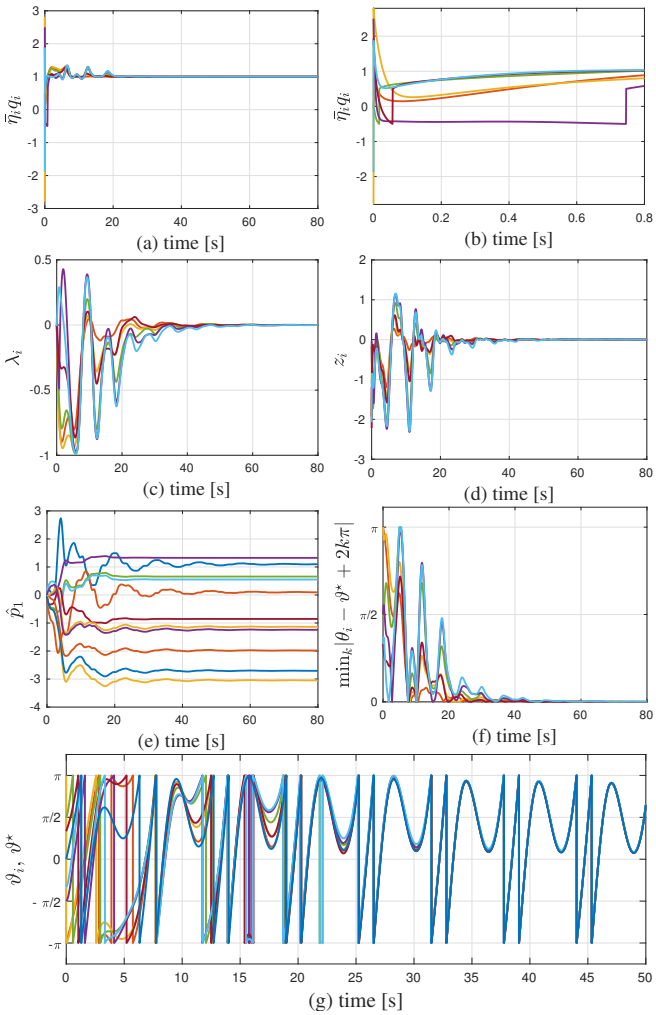

Fig. 7. Closed-loop simulation results. (a): phase tracking errors; (b): phase tracking errors, zoomed in $[\mathbf{0}, \mathbf{0.8}]$s to highlight the jumps during the initial transient; (c): filtered inputs $\boldsymbol{\lambda_i}$; (d): frequency tracking errors $\boldsymbol{z_i}$; (e): evolution of $\boldsymbol{\hat{p}_1}$; (f): arc distance between $\boldsymbol{\theta_i}$ and $\boldsymbol{\vartheta^\star}$; (g): phase angles, wrapped in the interval $[-\boldsymbol{\pi}, \boldsymbol{\pi})$ (reference in blue).

[12] G. S. Schmidt, A. Papachristodoulou, U. Münz, and F. Allgöwer, "Frequency synchronization and phase agreement in Kuramoto oscillator networks with delays," *Automatica*, vol. 48, no. 12, pp. 3008 – 3017, 2012.

[13] J. Zhang and J. Zhu, "Exponential synchronization of the high-dimensional Kuramoto model with identical oscillators under digraphs," *Automatica*, vol. 102, pp. 122 – 128, 2019.

[14] N. Chopra and M. W. Spong, "On exponential synchronization of Kuramoto oscillators," *IEEE Transactions on Automatic Control*, vol. 54, no. 2, pp. 353–357, Feb 2009.

[15] F. Dörfler and F. Bullo, "On the critical coupling for Kuramoto oscillators," *SIAM Journal on Applied Dynamical Systems*, vol. 10, no. 3, pp. 1070–1099, 2011.

[16] C. A. Moreira and M. A. de Aguiar, "Global synchronization of partially forced Kuramoto oscillators on networks," *Physica A: Statistical Mechanics and its Applications*, vol. 514, pp. 487 – 496, 2019.

[17] L. Zhu and D. J. Hill, "Synchronization of Kuramoto oscillators: A regional stability framework," *IEEE Transactions on Automatic Control*, vol. 65, no. 12, pp. 5070–5082, 2020.

[18] J. W. Simpson-Porco, F. Dörfler, and F. Bullo, "Synchronization and power sharing for droop-controlled inverters in islanded microgrids," *Automatica*, vol. 49, no. 9, pp. 2603–2611, 2013.

[19] R. Sepulchre, D. A. Paley, and N. E. Leonard, "Stabilization of planar collective motion: All-to-all communication," *IEEE Transactions on Automatic Control*, vol. 52, no. 5, pp. 811–824, 2007.

[20] ——, "Stabilization of planar collective motion with limited commu-

nication," *IEEE Transactions on Automatic Control*, vol. 53, no. 3, pp. 706–719, 2008.

[21] C. G. Mayhew, R. G. Sanfelice, J. Sheng, M. Arcak, and A. R. Teel, "Quaternion-based hybrid feedback for robust global attitude synchronization," *IEEE Transactions on Automatic Control*, vol. 57, no. 8, pp. 2122–2127, 2011.

[22] H. Gui and A. H. de Ruiter, "Global finite-time attitude consensus of leader-following spacecraft systems based on distributed observers," *Automatica*, vol. 91, pp. 225–232, 2018.

[23] Y. Wang and F. J. Doyle, "Exponential synchronization rate of Kuramoto oscillators in the presence of a pacemaker," *IEEE Transactions on Automatic Control*, vol. 58, no. 4, pp. 989–994, April 2013.

[24] L. Scardovi, A. Sarlette, and R. Sepulchre, "Synchronization and balancing on the N-torus," *Systems and Control Letters*, vol. 56, pp. 335–341, 2007.

[25] S. De Marco, L. Marconi, T. Hamel, and R. Mahony, "Output regulation on the special Euclidean group SE(3)," in *2016 IEEE 55th Conference on Decision and Control (CDC)*. IEEE, 2016, pp. 4734–4739.

[26] R. Mahony, T. Hamel, and J.-M. Pflimlin, "Nonlinear complementary filters on the special orthogonal group," *IEEE Transactions on Automatic Control*, vol. 53, no. 5, pp. 1203–1218, 2008.

[27] C. G. Mayhew, R. G. Sanfelice, and A. R. Teel, "Quaternion-based hybrid control for robust global attitude tracking," *IEEE Transactions on Automatic control*, vol. 56, no. 11, pp. 2555–2566, 2011.

[28] P. Casau, C. G. Mayhew, R. G. Sanfelice, and C. Silvestre, "Robust global exponential stabilization on the n-dimensional sphere with applications to trajectory tracking for quadrotors," *Automatica*, vol. 110, p. 108534, 2019.

[29] C. G. Mayhew and A. R. Teel, "Hybrid control of planar rotations," in *Proceedings of the 2010 American Control Conference*. IEEE, 2010, pp. 154–159.

[30] R. Goebel, R. G. Sanfelice, and A. R. Teel, *Hybrid Dynamical Systems: Modeling Stability, and Robustness*. Princeton University Press, Princeton, NJ, 2012.

[31] M. Maggiore, M. Sassano, and L. Zaccarian, "Reduction theorems for hybrid dynamical systems," *IEEE Transactions on Automatic Control*, vol. 64, no. 6, pp. 2254–2265, 2018.

[32] H. Cai and J. Huang, "Leader-following attitude consensus of multiple rigid body systems by attitude feedback control," *Automatica*, vol. 69, pp. 87–92, 2016.

[33] A. Isidori, *Nonlinear control systems II*. Springer, 1999.

[34] D. Invernizzi, M. Lovera, and L. Zaccarian, "Global robust attitude tracking with torque disturbance rejection via dynamic hybrid feedback," *Automatica*, vol. 144, p. 110462, 2022.

[35] R. G. Sanfelice and A. R. Teel, "Lyapunov analysis of sample-and-hold hybrid feedbacks," in *Proceedings of the 45th IEEE Conference on Decision and Control*. IEEE, 2006, pp. 4879–4884.

[36] A. Bosso, I. A. Azzollini, S. Baldi, and L. Zaccarian, "A hybrid distributed strategy for robust global phase synchronization of second-order Kuramoto oscillators," in *2021 IEEE 60th Conference on Decision and Control (CDC)*. IEEE, 2021.

[37] H. Zhang and F. L. Lewis, "Adaptive cooperative tracking control of higher-order nonlinear systems with unknown dynamics," *Automatica*, vol. 48, no. 7, pp. 1432–1439, 2012.

[38] R. G. Sanfelice and A. R. Teel, "On singular perturbations due to fast actuators in hybrid control systems," *Automatica*, vol. 47, no. 4, pp. 692–701, 2011.

[39] R. Goebel, R. G. Sanfelice, and A. R. Teel, "Hybrid dynamical systems," *IEEE Control Systems Magazine*, vol. 29, no. 2, pp. 28–93, 2009.

[40] P. A. Ioannou and J. Sun, *Robust Adaptive Control*, 1996.

[41] A. Bosso, I. A. Azzollini, and S. Baldi, "Global frequency synchronization over networks of uncertain second-order Kuramoto oscillators via distributed adaptive tracking," in *2019 IEEE 58th Conference on Decision and Control (CDC)*. IEEE, 2019, pp. 1031–1036.

[42] C. G. Mayhew, R. G. Sanfelice, and A. R. Teel, "On path-lifting mechanisms and unwinding in quaternion-based attitude control," *IEEE Transactions on Automatic Control*, vol. 58, no. 5, pp. 1179–1191, 2012.

[43] A. Isidori, L. Marconi, and G. Casadei, "Robust output synchronization of a network of heterogeneous nonlinear agents via nonlinear regulation theory," *IEEE Transactions on Automatic Control*, vol. 59, no. 10, pp. 2680–2691, 2014.

[44] I. A. Azzollini, W. Yu, S. Yuan, and S. Baldi, "Adaptive leader-follower synchronization over heterogeneous and uncertain networks of linear systems without distributed observer," *IEEE Transactions on Automatic Control*, 2020.

[45] A. Isidori, L. Marconi, and A. Serrani, *Robust Autonomous Guidance: an Internal Model Approach*. Springer Science & Business Media, 2012.

[46] H. K. Khalil, *Nonlinear Systems*, 3rd ed. Prentice Hall, 2002.

[47] M. Arcak and A. Teel, "Input-to-state stability for a class of Lurie systems," *Automatica*, vol. 38, no. 11, pp. 1945–1949, 2002.